



OSU LUNAR DOPPLER EXPERIMENT

W. H. Peake, R. H. Turpin and R. C. Taylor

The Ohio State University

ElectroScience Laboratory

(formerly Antenna Laboratory)

Department of Electrical Engineering
Columbus, Ohio 43212

REPORT 1388-22
1 August 1967

Grant Number NsG-213-61

(THRU)	1	(CODE)	07	(CATEGORY)
--------	---	--------	----	------------

N67 35462	(ACCESSION NUMBER)	77	(PAGES)	✓	(NASA CR OR TMX OR AD NUMBER)
-----------	--------------------	----	---------	---	-------------------------------

FACILITY FORM 602

National Aeronautics and Space Administration
Office of Grants and Research Contracts
Washington, D. C. 20546

NOTICES

When Government drawings, specifications, or other data are used for any purpose other than in connection with a definitely related Government procurement operation, the United States Government thereby incurs no responsibility nor any obligation whatsoever, and the fact that the Government may have formulated, furnished, or in any way supplied the said drawings, specifications, or other data, is not to be regarded by implication or otherwise as in any manner licensing the holder or any other person or corporation, or conveying any rights or permission to manufacture, use, or sell any patented invention that may in any way be related thereto.

The Government has the right to reproduce, use, and distribute this report for governmental purposes in accordance with the contract under which the report was produced. To protect the proprietary interests of the contractor and to avoid jeopardy of its obligations to the Government, the report may not be released for non-governmental use such as might constitute general publication without the express prior consent of The Ohio State University Research Foundation.

REPORT
by
THE OHIO STATE UNIVERSITY ELECTROSCIENCE LABORATORY
(Formerly Antenna Laboratory)
COLUMBUS, OHIO 43212

Sponsor National Aeronautics and Space Administration
 Office of Grants and Research Contracts
 Washington, D. C. 20546

Grant Number NsG-213-61

Investigation of Theoretical and Experimental Analysis of the
 Electromagnetic Scattering and Radiative
 Properties of Terrain, with Emphasis on
 Lunar-Like Surfaces

Subject of
Report OSU Lunar Doppler Experiment

Submitted by W. H. Peake, R. H. Turpin and R. C. Taylor
 ElectroScience Laboratory
 Department of Electrical Engineering

Date 1 August 1967

ABSTRACT

This report describes an S-band cw Doppler lunar radar experiment conducted at The Ohio State University ElectroScience Laboratory. The results for the scattering function, total cross section and surface properties are compared with experimental results of other investigators and with recent theoretical interpretations.

CONTENTS

	Page
I. INTRODUCTION	1
II. THE DOPPLER EXPERIMENT	1
III. INSTRUMENTATION	4
IV. DATA	5
V. DATA ANALYSIS	9
VI. ACCURACY OF MEASUREMENTS	31
VII. CONCLUSIONS	33
VIII. RECOMMENDATIONS FOR FUTURE WORK	33
REFERENCES	34
ACKNOWLEDGEMENTS	35
APPENDIX	
A Completion of "The Solution of an Integral Equation for the Lunar Scattering Function"	36
B Empirical $P(f) - \sigma_0(\alpha)$ Pairs	38
C Discussion of Receiver Setup	42
D Calculation of Doppler Shift and Doppler Smear of Lunar Radar Echos	44
E Scatran Computer Programs (Compatible with the OSU IBM 7094 Computer) for Data Analysis	63
F Suggestions for Efficient Digital Spectral Analysis	74

OSU LUNAR DOPPLER EXPERIMENT

I. INTRODUCTION

The use of radar as a means for studying remote surfaces (such as planetary surfaces) has been the object of both theoretical and experimental work for a number of years, and has assumed an increasingly important role in the study of our solar system. Recent¹ radar studies of Venus, for example, have significantly improved on the knowledge of our nearest planetary neighbor. The interpretation of these radar studies, however, is not yet entirely well founded. The moon, being relatively close to the Earth, can serve to verify some of these interpretations.

This report describes an S-band CW Doppler lunar radar experiment conducted at The Ohio State University ElectroScience Laboratory during 1965. The results for the scattering function, total cross section and surface properties (dielectric constant and effective RMS slope) are compared with experimental results of other investigators and with the theoretical interpretations of References 2 and 3.

II. THE DOPPLER EXPERIMENT

The moon's orbital motion imposes two kinds of Doppler effects on a radar signal incident on its surface. The first (Fig. 1) is an overall Doppler shift, f_D , due to the motion of the center of the moon relative to the center of the earth. This continuously changing frequency shift must be accurately known in order to "track" the reflected signal in frequency.

A second kind of Doppler effect arises from the apparent libration, or rotation, of the moon. This is the foundation of the "Doppler experiment". The effect of this libration is to smear the spectrum of the transmitted signal in accordance with the Doppler principle. This smeared spectrum is shown in Fig. 1, where the maximum Doppler smear, f_{dmax} , corresponds to the return from the limb of the moon.

The major source of the apparent libration is the rotation of the Earth. A second source, producing a libration in latitude, is the inclination of the moon's equator to its orbital plane. Finally, the

slight eccentricity of the moon's orbit coupled with a constant axial rotation produces a longitudinal libration.

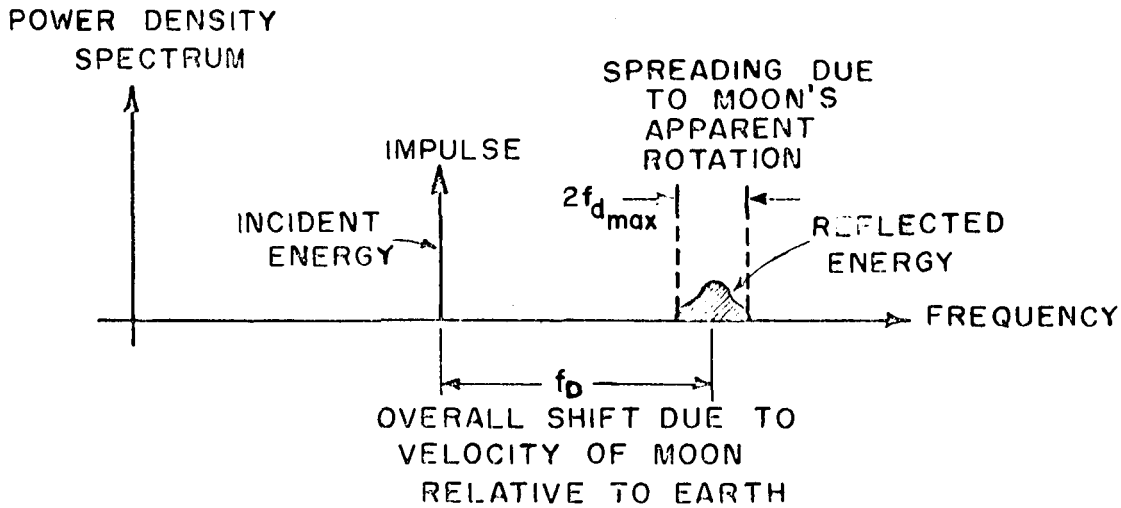


Fig. 1. Frequency behavior of lunar echo.

In Reference 4 it is shown that, for the geometry of Fig. 2, all points on the surface of the moon with a given y-coordinate produce the same Doppler shift, given by the equation

$$(1) \quad f_d = \frac{2RfL}{c} \sin \phi,$$

where

R = radius of the moon (1738 km),
 c = velocity of light,
 f = transmitted frequency (2270 MHz) and
 L = total libration rate (radians/sec).

The angle ϕ is defined in Fig. 2. Thus there is a direct correspondence between Doppler strips on the moon and frequency bands in the spectra of moon-reflected radar signals.

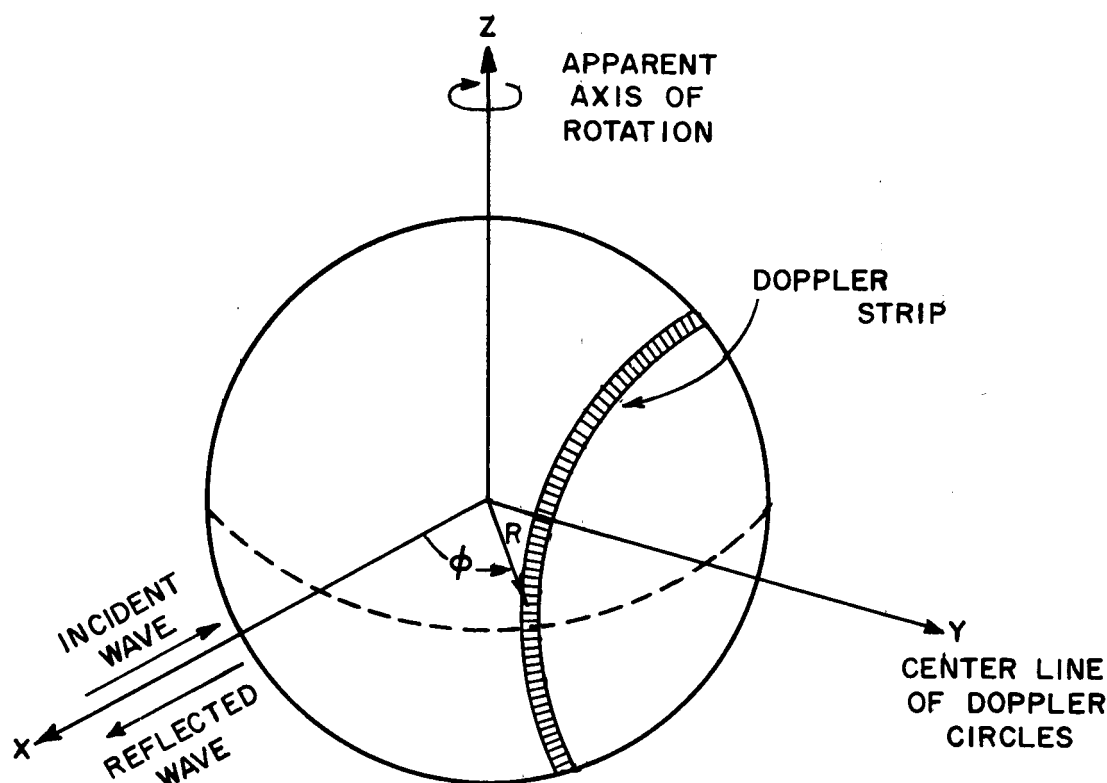


Fig. 2. Geometry of Doppler shift due to libration.

An average backscattering cross section per unit area $\sigma_o(\alpha)$, where α is the angle of incidence (see Fig. 3), can be computed from the Doppler derived power spectrum, $P(f)$, by numerical integration of the equation (see References 1, 4 and 12, and Appendix I)

$$(2) \quad \sigma_o(\alpha) = \frac{1}{\pi R} \cos \alpha \int_1^{\sin \alpha} \frac{P'(\xi)}{\sqrt{\xi^2 - \sin^2 \alpha}} d\xi,$$

where ξ is the normalized frequency, $\xi = \frac{f-f_D}{f_{d_{\max}}}$, $0 \leq \xi \leq 1$, and α

is the angle of incidence. The prime (') denotes the derivative with respect to ξ . Once $\sigma_0(\alpha)$ is known, the extensive literature for interpretation of surface structure in terms of the angular dependence of $\sigma_0(\alpha)$ may be used to obtain information about the lunar surface.

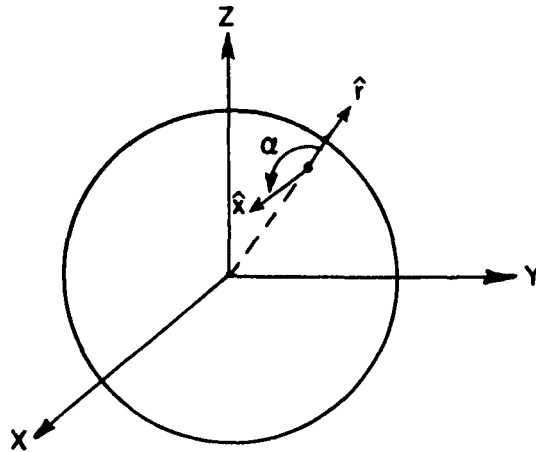


Fig. 3. Angle of incidence, α .

III. INSTRUMENTATION

The transmitted signal (2270 MHz at 10 kW) was derived from a Sulzer frequency standard and was provided by The Ohio University (30 ft paraboloidal antenna; $82^{\circ} 07' 29''$ W longitude, $39^{\circ} 19' 28''$ N latitude, 274 m elevation). Only linearly polarized signals were transmitted.

The receiving station was The Ohio State University ElectroScience Laboratory Satellite Communication Facility ($82^{\circ} 02' 30''$ W longitude, $40^{\circ} 00' 10''$ N latitude, 247 m elevation) using two of an array of four 30 ft paraboloidal antennas (1° beamwidth, 43 dB gain). Parametric amplifiers provided approximately 4 dB noise figures, 20 dB gain and 30 MHz bandwidth. Both direct- and cross-polarized signals were received.

The receiver system (Fig. 4) made use of the stability of the rubidium vapor frequency standard to perform direct recording of the lunar-reflected signals. The second local oscillator was offset and varied in accordance with computed values of overall Doppler shift to yield a final output center frequency of about 150 Hz or, for some data runs, about 90 Hz. The final downconverted signal was then recorded undetected on magnetic tape.

IV. DATA

Data runs were 10 to 15 minutes in length with 45 minutes between consecutive runs. Preceding each series of runs a frequency check was made of the transmitter-receiver system by direct transmission from Ohio University to The Ohio State University. Paramp gain and noise figure measurements were made for each series of runs. Immediately before or immediately following each run system noise levels and 0- to 1-volt calibration levels were recorded. All the data were FM-recorded on magnetic tape with a 1250 Hz bandwidth at $7\frac{1}{2}$ ips.

Figure 5(a) shows a sample of direct-polarized return received at 20:20 UT* on June 3, 1965 with 20 dB attenuation ahead of the receiver. A sample of cross-polarized return (with 8 dB attenuation), recorded at the same time, is shown in Fig. 5(b). Both the direct- and the cross-polarized data were normalized to the maximum value of the former within the interval plotted.

Examples of the probability density functions of the received signals are shown in Fig. 6. It is of interest to note the close approximation to the normal (Gaussian) distribution. This implies that very little of the return is coherent, as expected for radar return from a rough surface. The fact that the return was indeed found to be approximately Gaussian, can find application in some considerations of data analysis. An example of an analysis technique requiring a Gaussian amplitude distribution will be discussed briefly in Appendix F.

* Universal Time

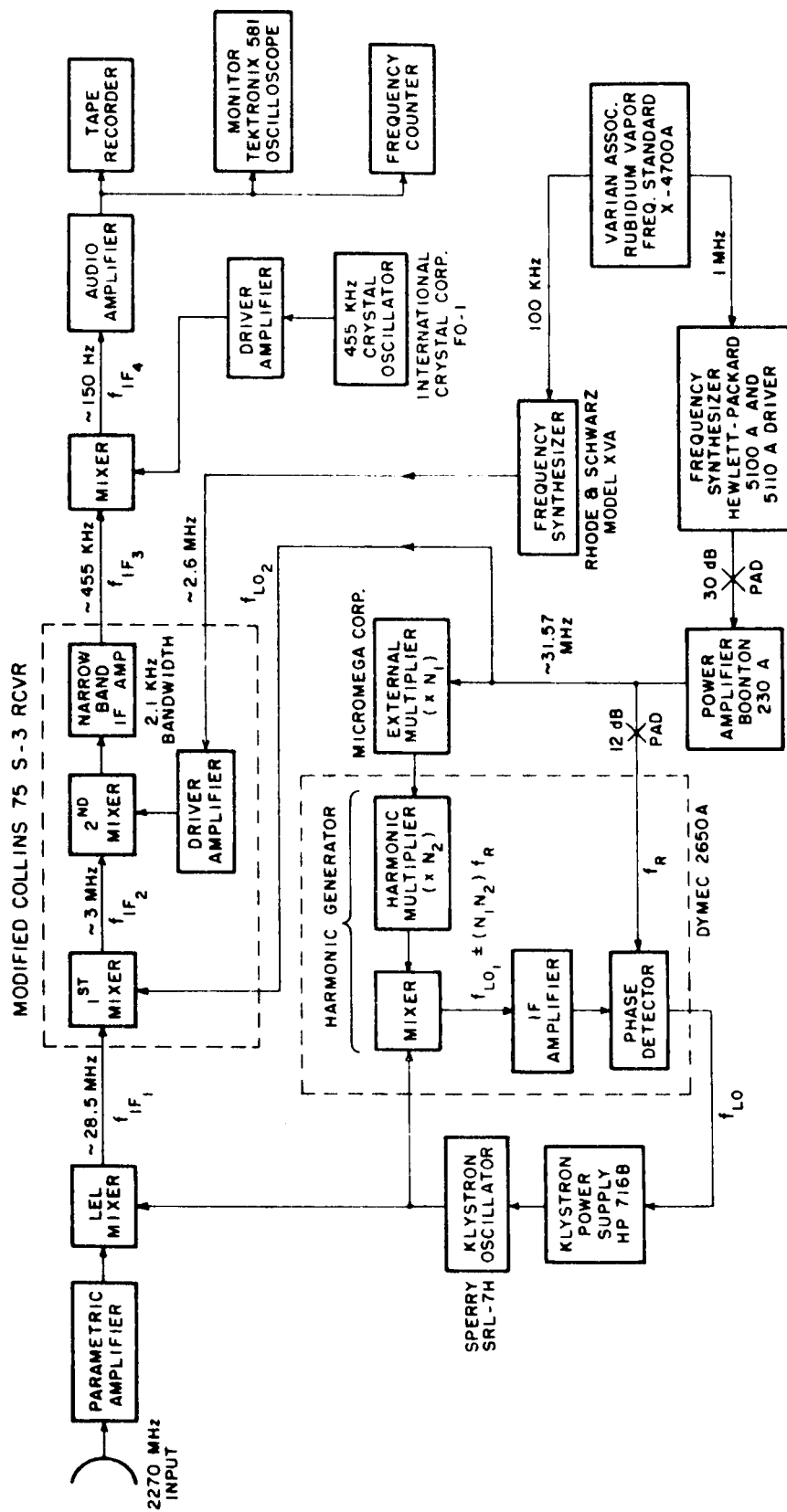


Fig. 4. OSU receiver system for lunar experiment.

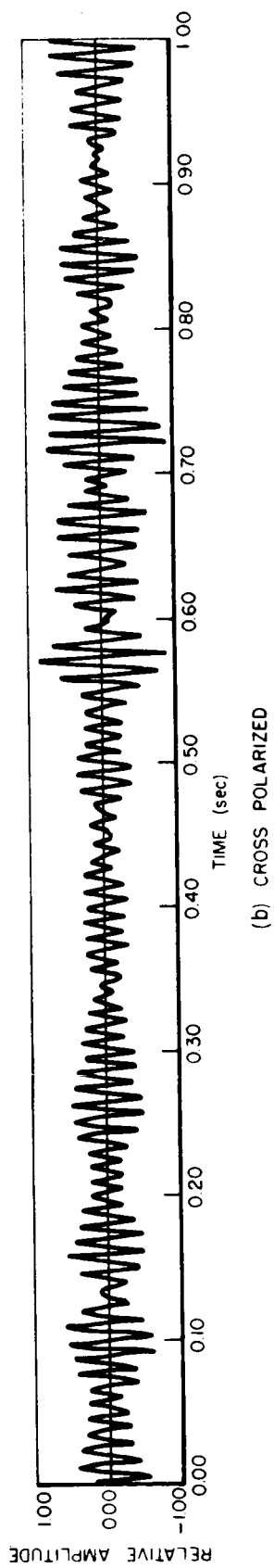
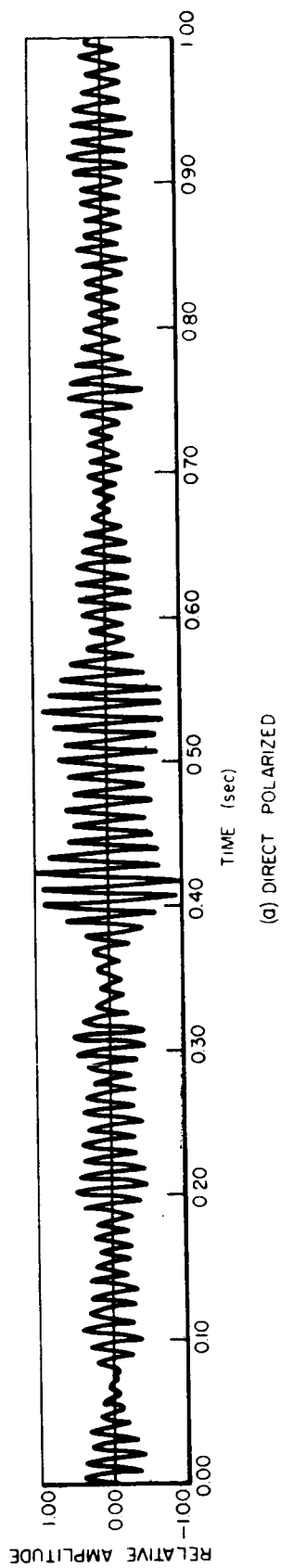


Fig. 5. Data samples.

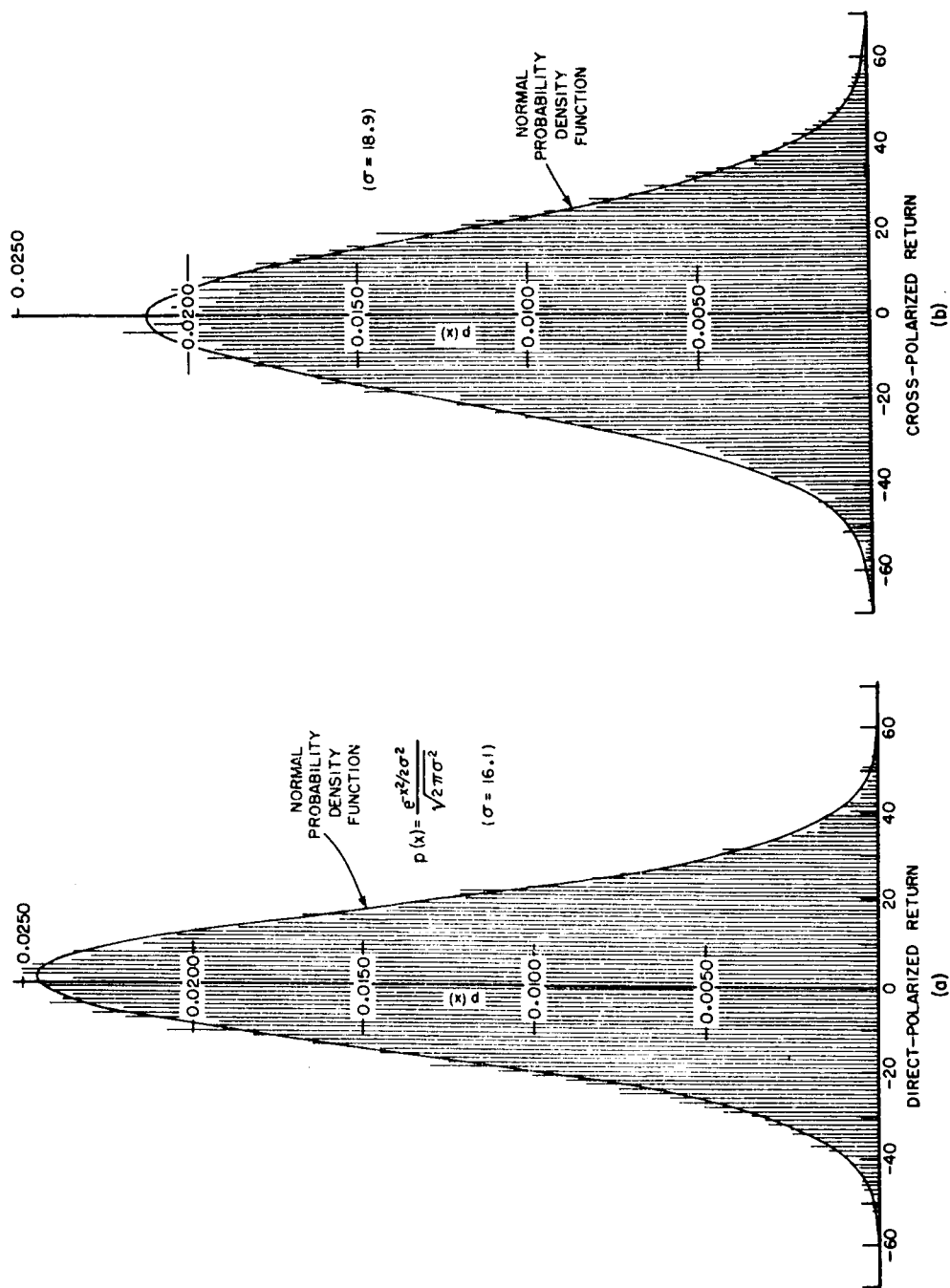


Fig. 6. Probability density functions
(19:58 UT, June 3, 1965).

Selected portions of the analog data were digitized, initially at Wright-Patterson Air Force Base (WPAFB) and later at The Ohio State University Computer Center. At WPAFB the data were digitized with a sample rate of 1250 samples per second and a bandwidth of 1250 Hz. Because the signal bandwidth was no greater than 180 Hz, this was an excessive sample rate. To reduce the sample rate and, at the same time, the noise bandwidth, the smoothing^{5,6} and "decimation" operator $F_2S_2S_3^*$ was applied, yielding an apparent sample rate of 625 samples per second and a half-power bandwidth of a little less than 180 Hz. Figure 7 shows the power transfer loss corresponding to the smoothing operator S_2S_3 . The spectra computed from these modified data were appropriately corrected, as discussed in the following section.

More data were digitized following the installation of an analog-to-digital converter at the OSU Computer Center. With this new and convenient facility greater control of playback bandwidth and sample rate was possible. A more suitable sample rate of 500 samples per second was chosen. In order to realize a bandwidth sufficiently narrow to avoid data contamination by the spectral "folding" inherent in the sampling process, and thus to avoid the need for data smoothing, it was necessary to play back the analog data at a $1\frac{3}{4}$ ips rate, yielding a bandwidth of about 312.5 Hz. Figure 8 illustrates the reasoning behind this choice of parameters.

V. DATA ANALYSIS

The power spectrum, from which the backscattering function is computed, is derived from the autocovariance function (ACF) of the data. The ACF of digitized data is defined^{5,6} by the expression

$$C_r = \frac{1}{N-r} \sum_{i=0}^{N-r} x_i x_{i+r}, \quad r = 0, 1, \dots, m,$$

where $N + 1$ is the total number of data points (x_0, x_1, \dots, x_N) , m corresponds to the maximum covariance lag $\tau_m = m\Delta t$ ($1/\Delta t$ is the sample rate) and C_r is the r^{th} term of the autocovariance function, corresponding to a lag of $r\Delta t$. A maximum covariance lag of 1 second

* The notation is that of Blackman and Tukey (Ref. 5) for convenience.

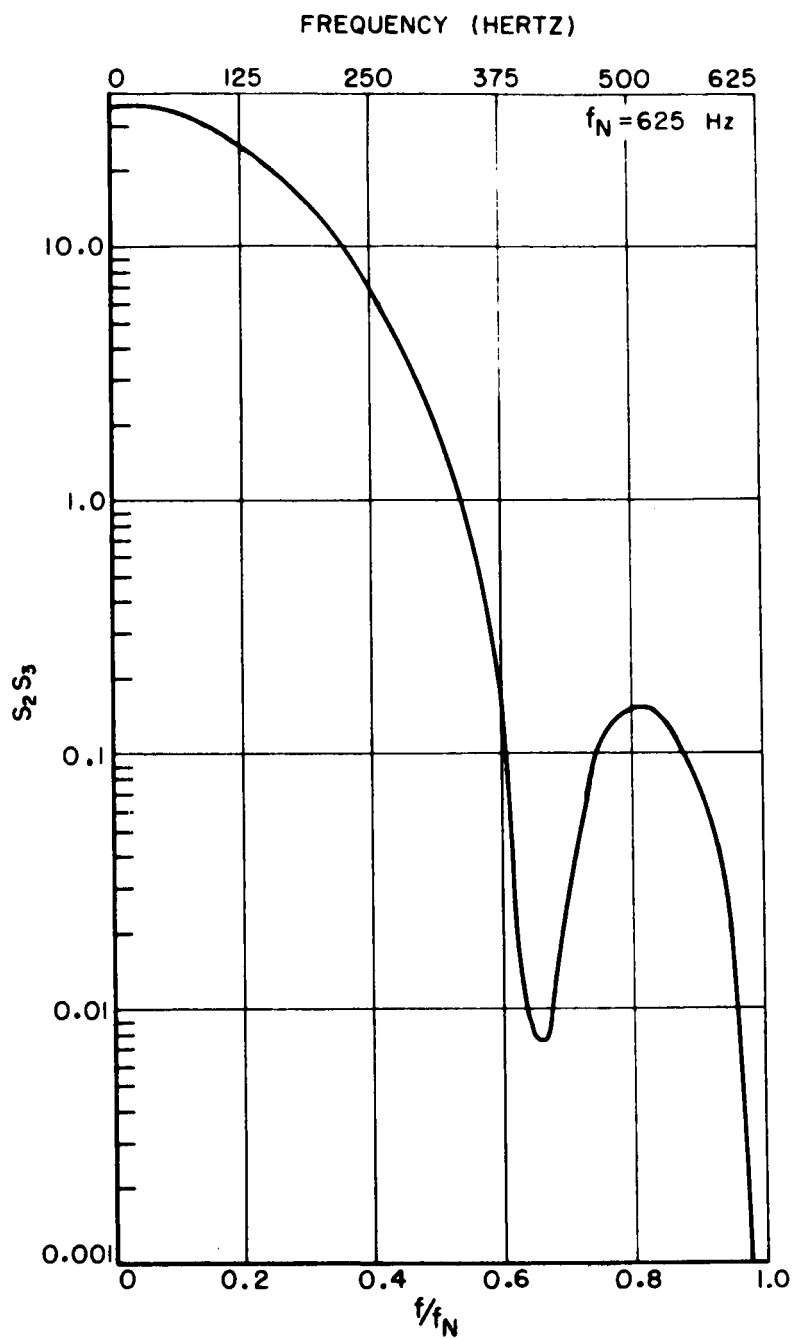


Fig. 7. Power transfer ratio for smoothing operator, $S_2 S_3$.

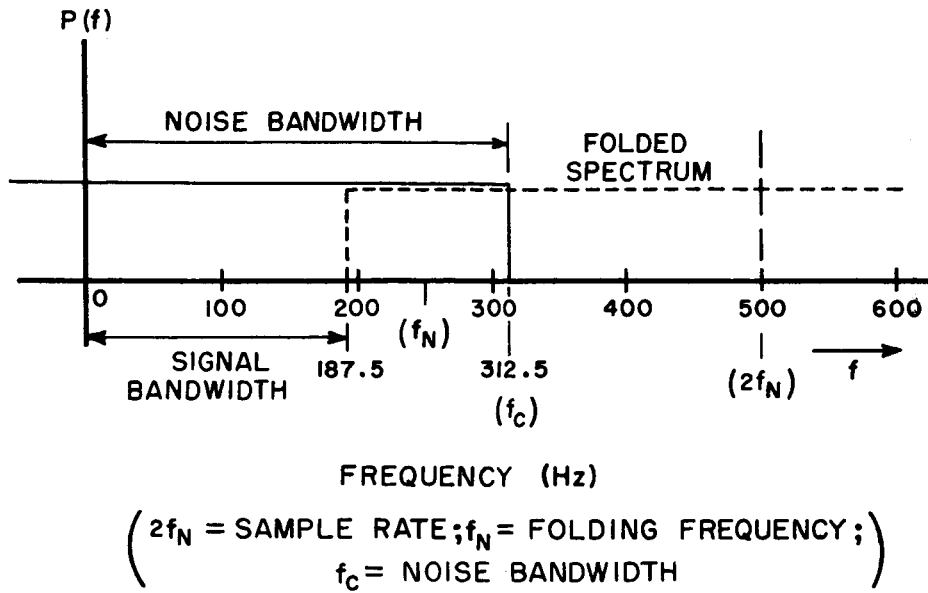


Fig. 8. Determination of sampling rate.

was used in order to obtain a 1 Hertz resolution in the power spectra. An example of an ACF is shown in Fig. 9.

A rough spectral density estimate was derived from each ACF by the formula^{5,6}

$$(4) \quad V_r = \Delta t \left[C_0 + 2 \sum_{i=1}^{m-1} C_i \cos \frac{ir\pi}{m} + C_m \cos r\pi \right]$$

for $r = 0, 1, \dots, m$. The frequency corresponding to r is $\frac{r}{2m\Delta t}$ Hz.

The rough spectral estimates derived from the WPAFB-digitized data were corrected for the smoothing function, $S_2 S_3$, by multiplying the spectra by the inverse function^{5,6}

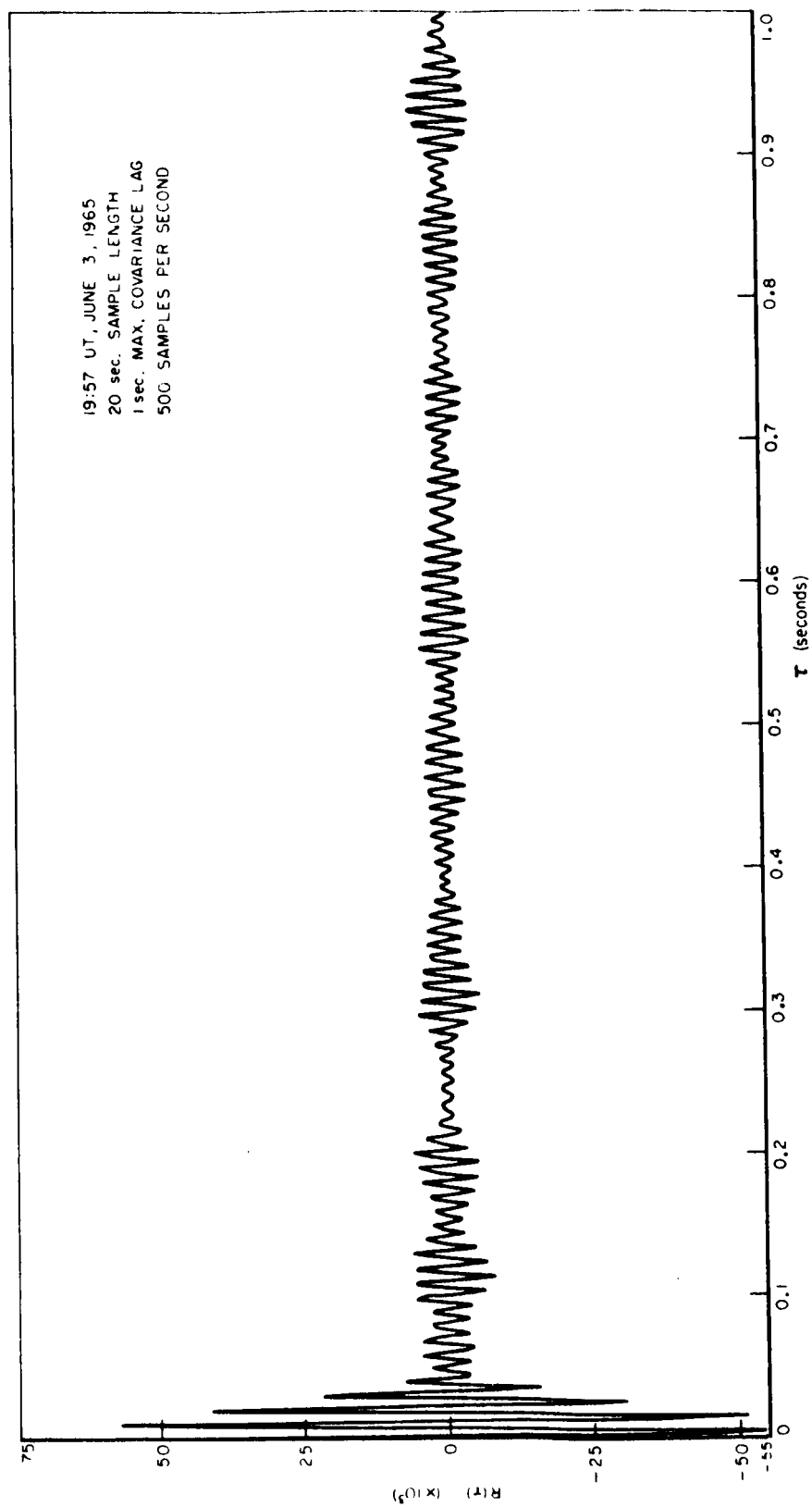


Fig. 9. Autocovariance function.

$$(5) \quad \left(\frac{\sin \frac{\omega \Delta t}{2}}{\sin \frac{2\omega \Delta t}{2}} \right)^2 \left(\frac{\sin \frac{\omega \Delta t}{2}}{\sin \frac{3\omega \Delta t}{2}} \right)^2 ,$$

where $\omega = 2\pi f$ and $\frac{1}{\Delta t}$ is the sample rate.

These rough spectral estimates were then smoothed^{5,6} by Hanning weights in the manner shown here to produce final estimates U_r .

$$U_0 = 0.5 U_0 + 0.5 U_1,$$

$$(6) \quad U_r = 0.25 U_{r-1} + 0.5 U_r + 0.25 U_{r+1}, \quad r = 1, 2, \dots, m-1,$$

$$U_m = 0.5 U_{m-1} + 0.5 U_m.$$

In Reference 5, formulas are given which may be used to estimate the amount of data required to obtain a certain precision in the spectral estimates. One example is the formula

$$(7) \quad N = \frac{\frac{1}{2} + \frac{200}{(90 \text{ per cent range in dB})^2}}{(L)(R) - \frac{1}{3}},$$

where N is the number of pieces of data, L is the length (in seconds) of each piece, and R is the desired frequency resolution in Hertz. The expression "90 per cent range in dB" is explained as follows. A "spectral estimate" is composed of a number of individual estimates of the spectral densities at discrete frequencies. Consider a set of M such "spectral estimates". Each member of the set includes an estimate of the spectral density at the discrete frequency f_n . There is thus a total of M independent estimates corresponding to f_n . The purpose of the statement "90 per cent range in dB" is to specify that 90 per cent of these M estimates will lie within a certain range (in dB) of the average of all M estimates for f_n . This specification applies to each frequency included in the spectral estimates.

For the data available in this experiment it was desired to obtain one Hertz resolution with data samples 20 seconds in length. The 90 per cent range was set at ± 2 dB. Applying the formula of Eq. (7) to these parameters gives

$$(8) \quad N = \frac{\frac{1}{2} + \frac{20}{(2)^2}}{(20)(1) - \frac{1}{3}} = \frac{50.5}{19.7} \sim 3.$$

Thus the average of spectral estimates derived from three 20 second data samples should provide a final spectral estimate satisfying the desired criteria.

Figure 10 presents a sample spectral estimate derived from 20 seconds of data recorded on May 4, 1965 at 23:14 UT. Figure 11 presents two 20 second spectra, one (a) from direct-polarized return and the other (b) from cross-polarized return. The data for these spectra were acquired at 20:20 UT on June 3, 1965. In both Fig. 10 and Fig. 11 intermodulation sidebands appear due to the presence of 60 Hertz in the receiver system. Since the signal spectra were less than 60 Hertz wide, however, they were not contaminated.

The spectral estimates from a number of runs are shown in Fig. 12. All are derived from 60 seconds of data, have one Hertz resolution and have been plotted against a normalized frequency variable $\xi = \frac{f-f_D}{f_{D_{\max}}}$. The values for $f_{D_{\max}}$, the limb Doppler, were determined both by a computer program (Appendix D) and by estimation directly from the spectral density curves.

The CW spectrum and the backscattering function of the moon are related (Ref. 4 and Appendix A, Ref. 1 and Ref. 12) by the following pair of equations

$$(9) \quad P(\xi) \propto \int_{\sin^{-1}\xi}^{\pi/2} \frac{\sigma_o(\alpha) \sin \alpha}{\sqrt{\sin^2 \alpha - \xi^2}} d\alpha$$

$$(10) \quad \sigma_o(\alpha) \propto \cos \alpha \int_1^{\sin \alpha} \frac{P'(\xi)}{\sqrt{\xi^2 - \sin^2 \alpha}} d\xi,$$

where $P(\xi)$, the spectral density function, is assumed even, differentiable, and frequency normalized so that $0 \leq \xi \leq 1$ (ξ is thus dimensionless). It is assumed that $\sigma_o(\alpha)$, the backscattering function, is a function only of the angle between the radius vector of the moon, \hat{r} , and the direction of incidence, \hat{x} (Fig. 3).

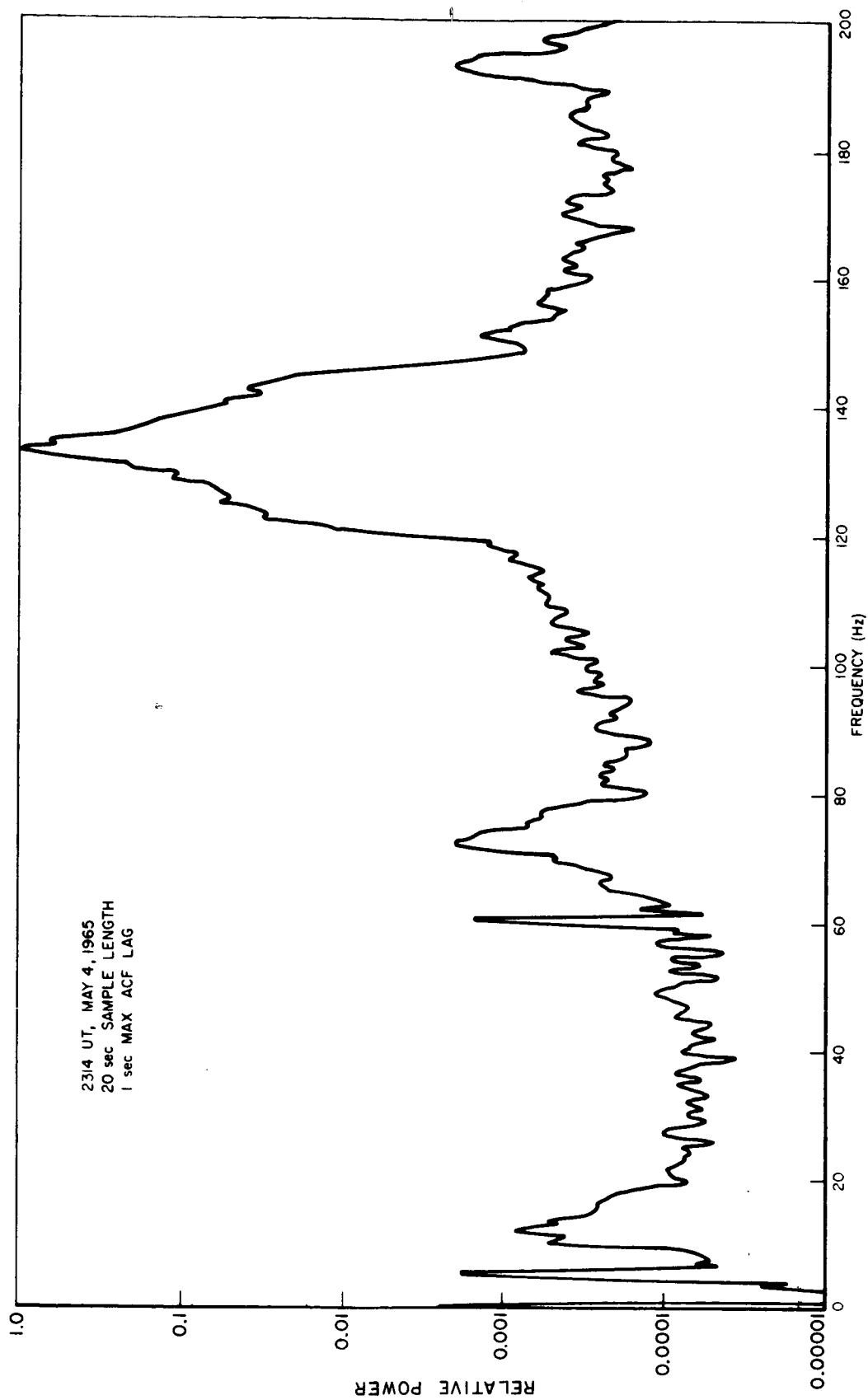


Fig. 10. Power spectral density function.

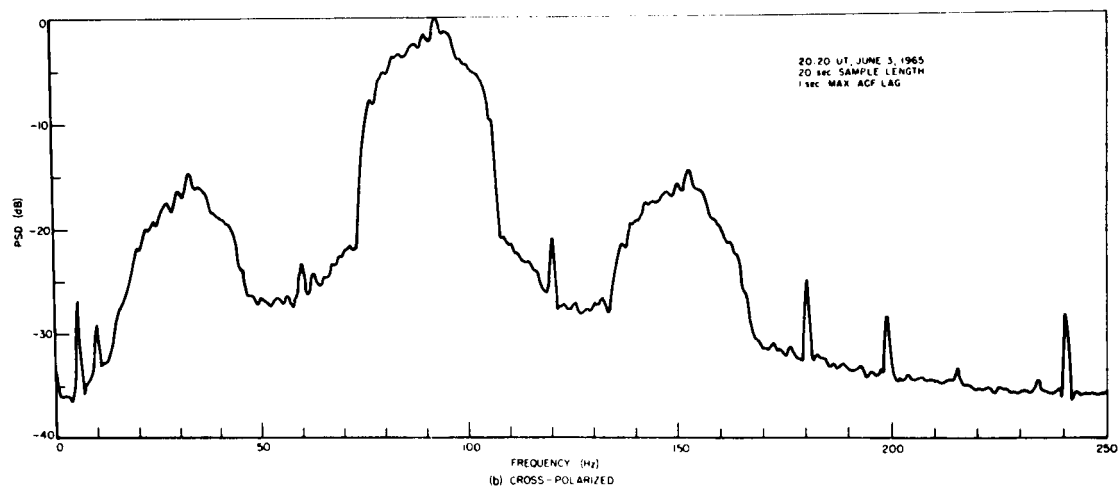
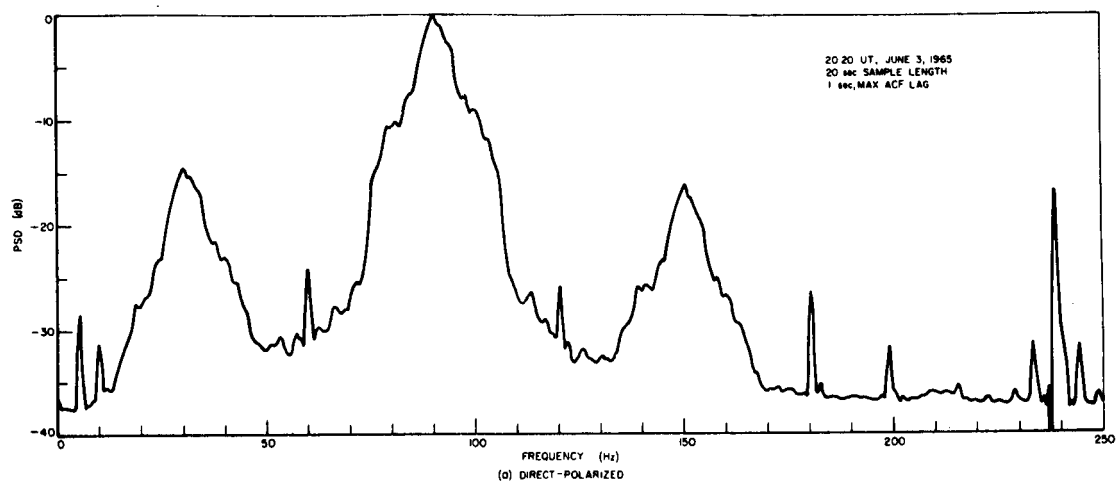


Fig. 11. Power spectral density functions.

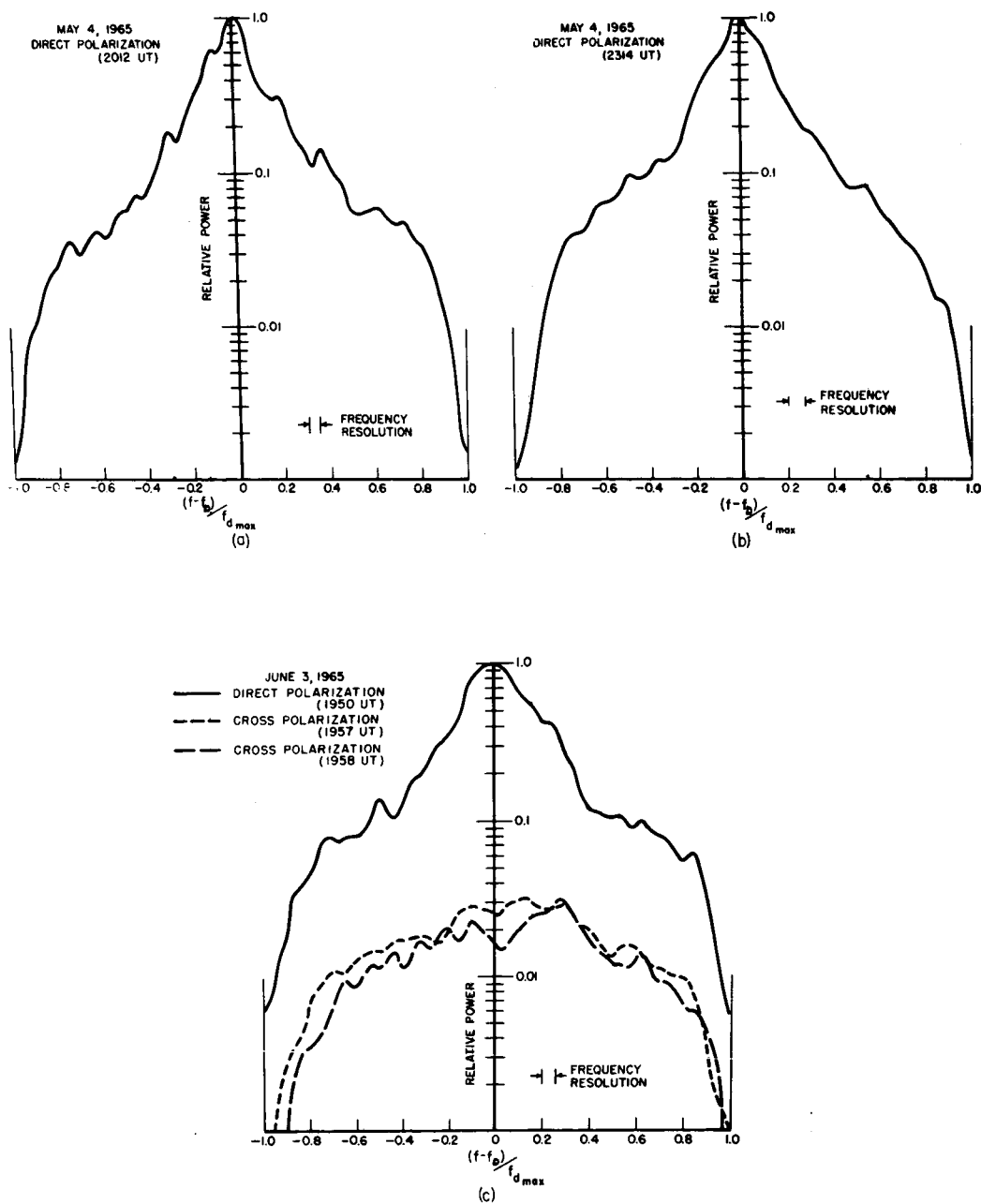


Fig. 12. Frequency-normalized spectral density functions.

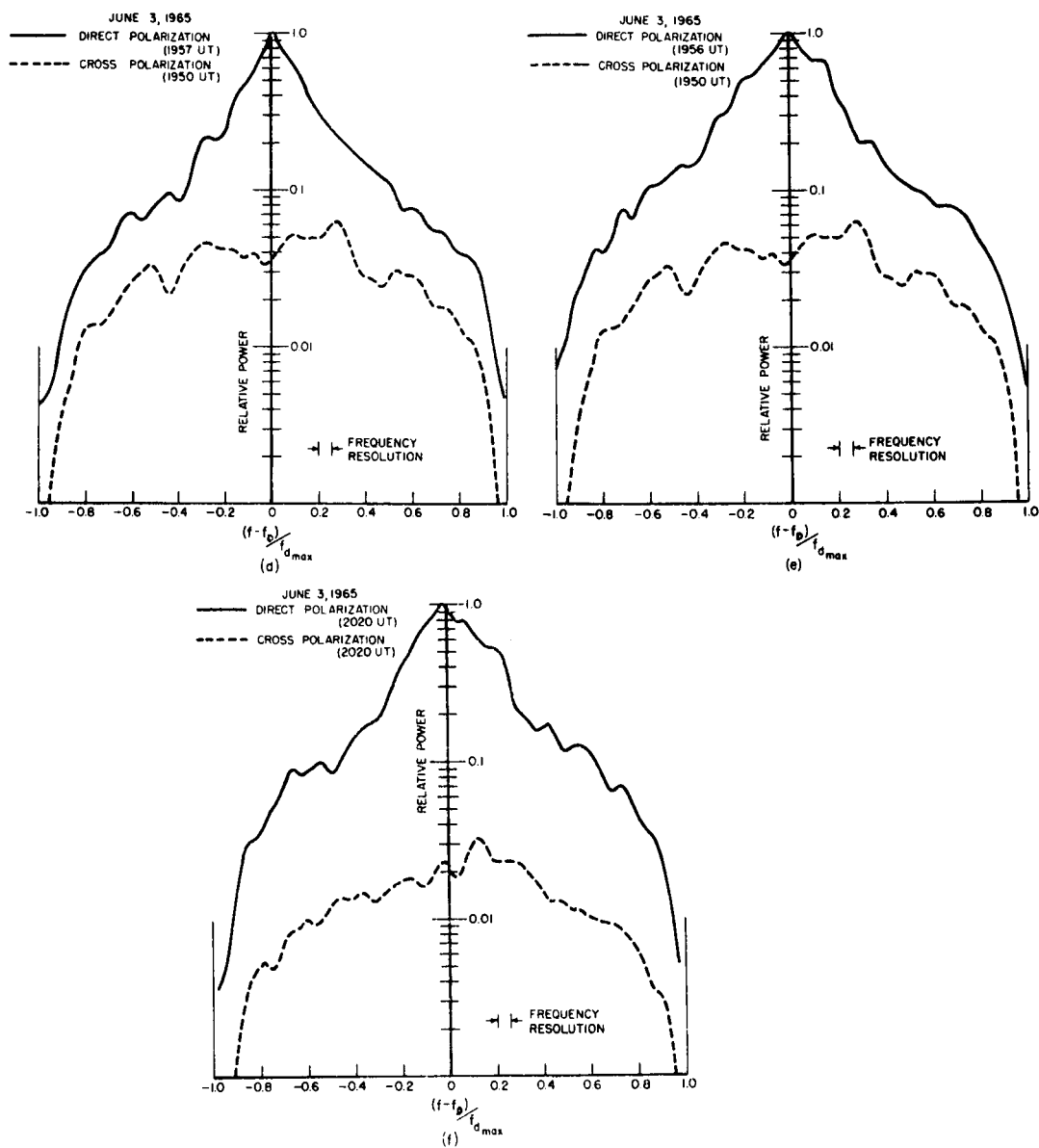


Fig. 12. Frequency-normalized spectral density functions.

The estimates of $\sigma_0(\alpha)$ derived, by numerical integration of Eq. (10), from the spectra of Fig. 12 were averaged to yield the functions shown in Fig. 13. Curves obtained^{9, 17} by other investigators at different wavelengths and with both linear and circular polarization are shown in Fig. 14 to provide a comparison. Direct comparison of linear- and circular-polarization results (Figs. 13 and 14, respectively) cannot be made,² though an approximate comparison is valid for angles of incidence near normal.

A comparison of the measured backscattering function (Fig. 13) with theoretically derived backscatter functions is shown in Fig. 15. In this instance the backscatter parameter $\gamma(\alpha) = \frac{\sigma_0(\alpha)}{\cos \alpha}$, is plotted rather than $\sigma_0(\alpha)$, to provide a direct comparison with the curves given in Reference 3. The curves have been normalized at the origin for this purpose. It may be concluded from this comparison that the RMS surface slope is about 15° at a wavelength of 13.2 cm. The disagreement between experimental and theoretical results for large angles of incidence is, at least in part, due to the failure of the physical optics approximation at these angles. A similar comparison (Fig. 16) of the experimental backscatter functions of other investigators with the theoretical curves of Reference 3, over a 0 to 20° range, provides an estimate of the frequency dependence of the RMS surface slope (see Fig. 17). As wavelength, λ , decreases, the effects of smaller surface features on the radar signal produce an increase in the apparent surface slope.

Comparison of these experimental results with the theoretical predictions of References 2 and 3 (see Fig. 15) also suggests that the modified Bessel joint probability density function^{2, 7} is a more accurate model for describing the lunar surface than is the Gaussian joint probability density function, for angles of incidence near normal.

The experimental cross-polarized backscattering parameter is compared with the corresponding theoretical^{2, 3} curve in Fig. 18. Both curves have been normalized to 0 dB at their maximum values. Little correlation is observed between the two curves. Part of the discrepancy is undoubtedly due to the lack of transmitter-receiver isolation, especially near normal incidence.

The experiment also provides information on the absolute cross-section of the moon. The total radar cross-section is defined by

$$(11) \quad \sigma = \pi r^2 g \rho = \frac{(4\pi)^3 d^4 P_r}{P_t G_t G_r \lambda^2} ,$$

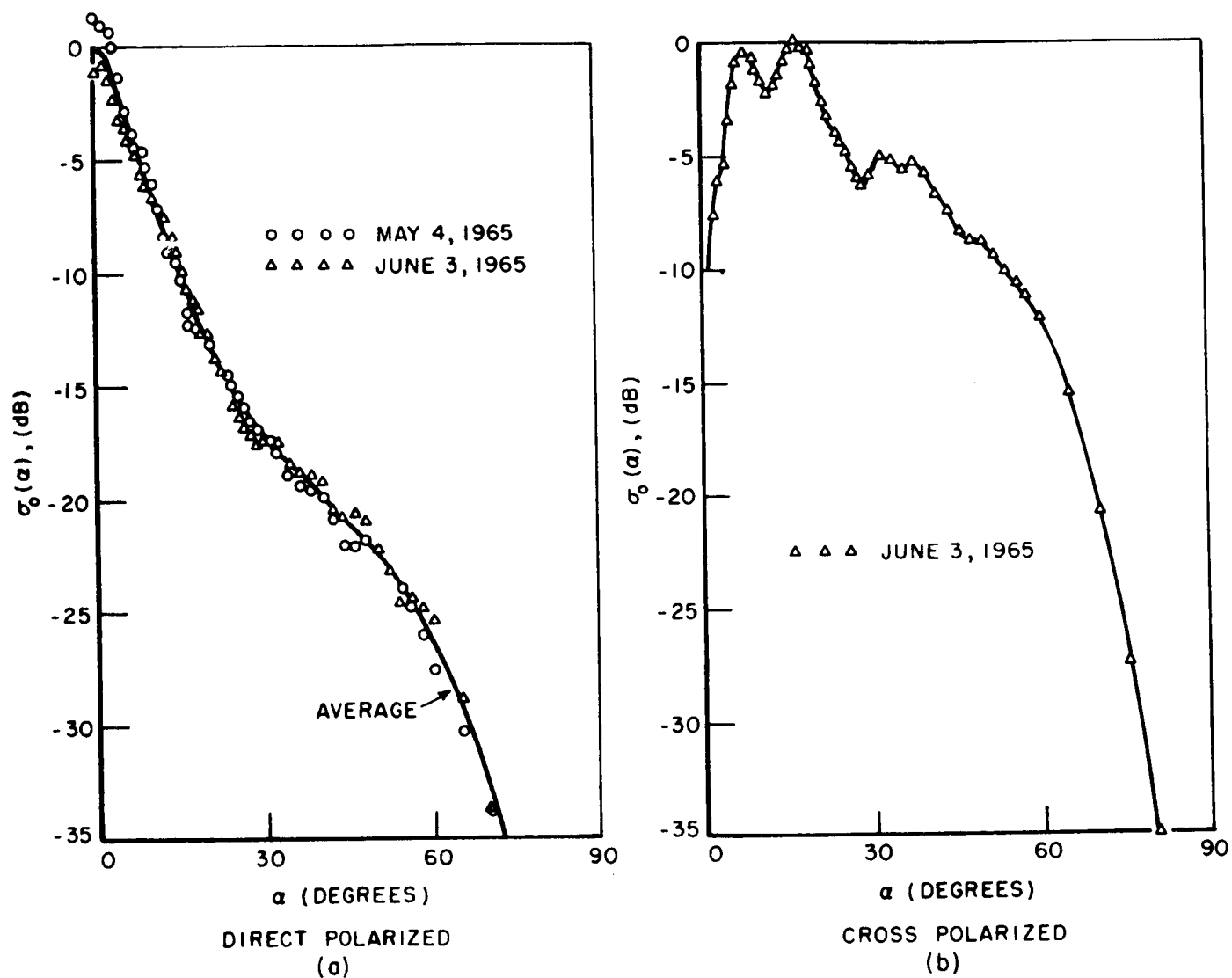


Fig. 13. Average backscattering cross section, linear polarization.

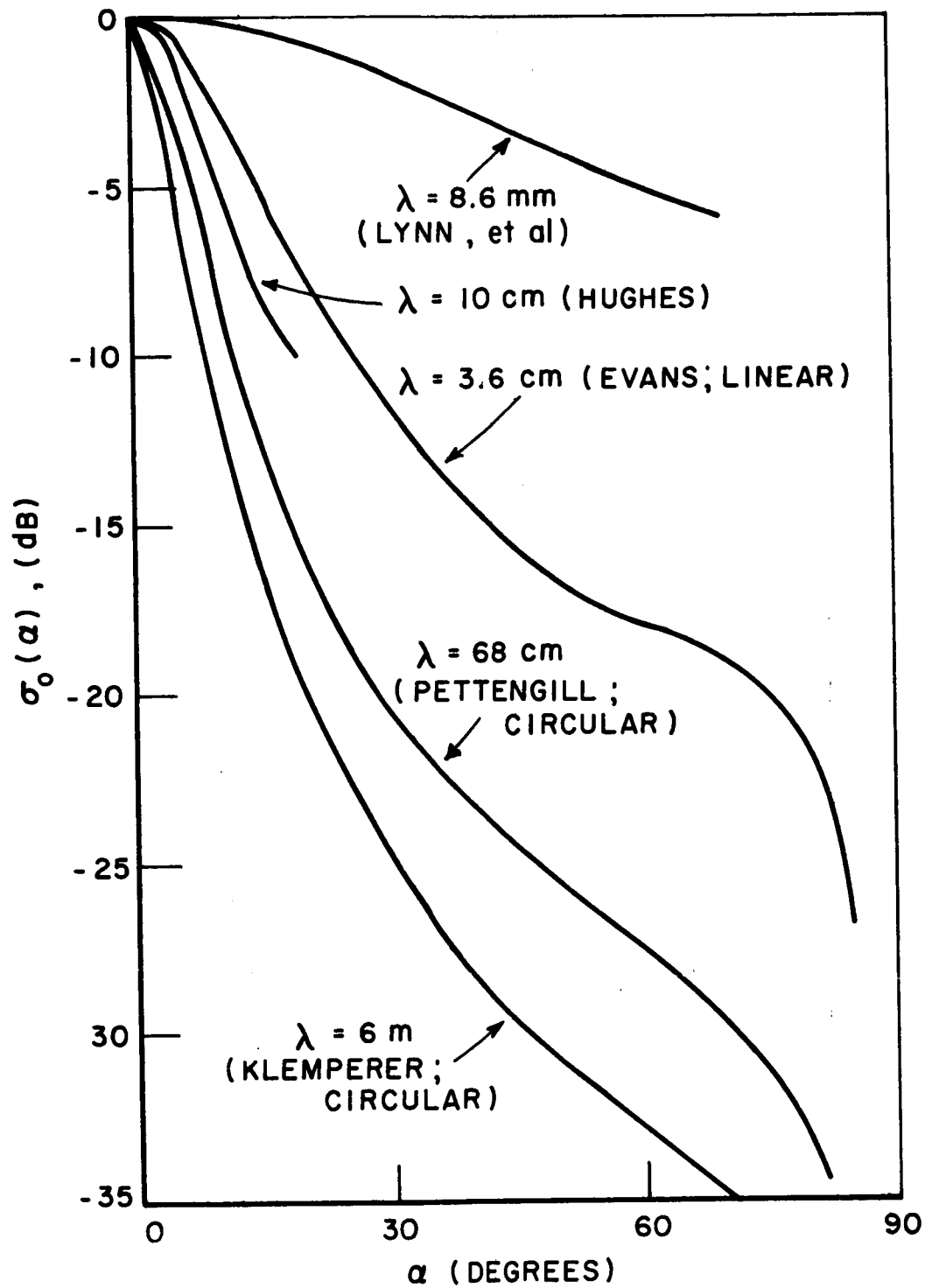


Fig. 14. Average backscattering cross section by other investigators (circular polarization).

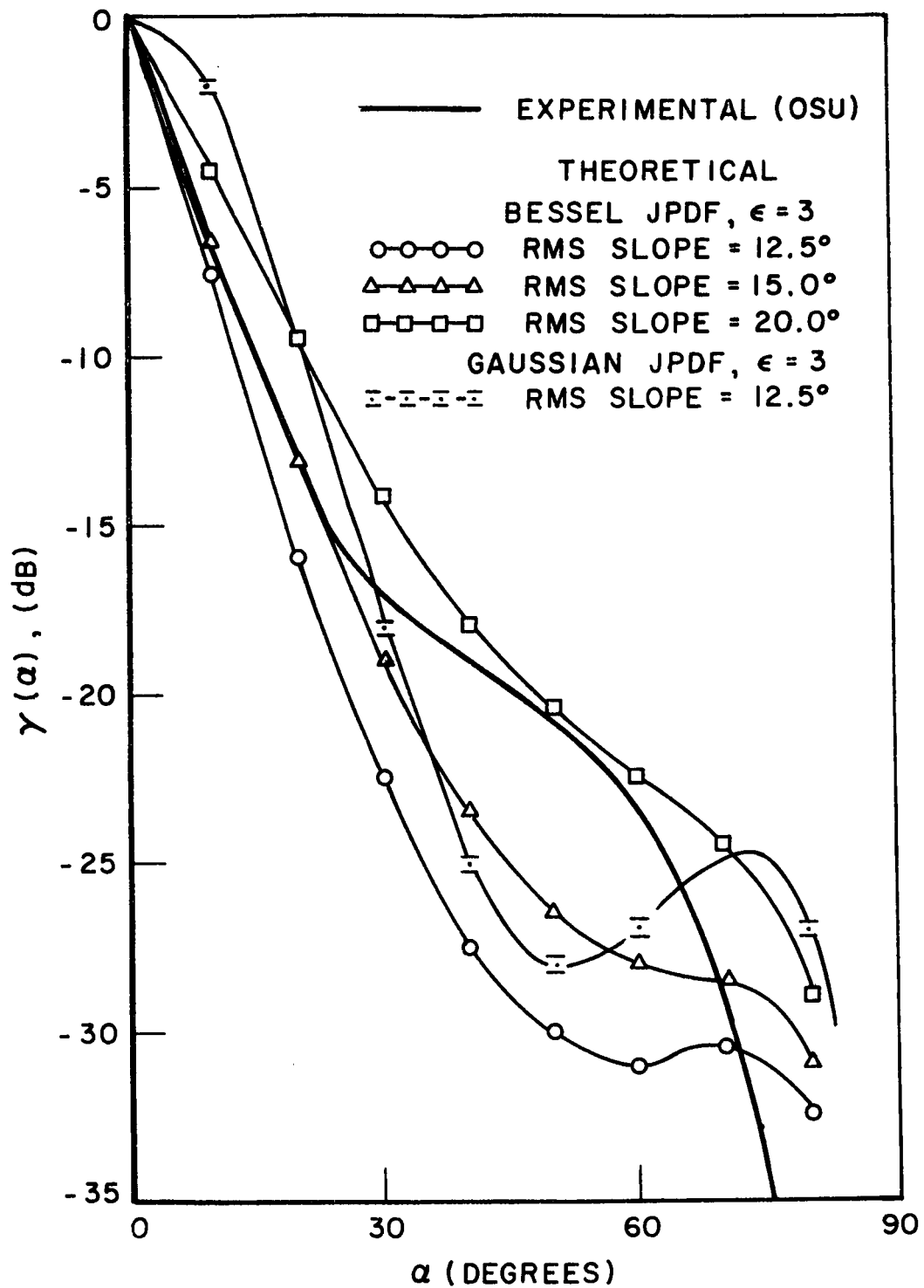


Fig. 15. Comparison of $\gamma(\alpha)$ with theoretical predictions (Ref. 2, 3).

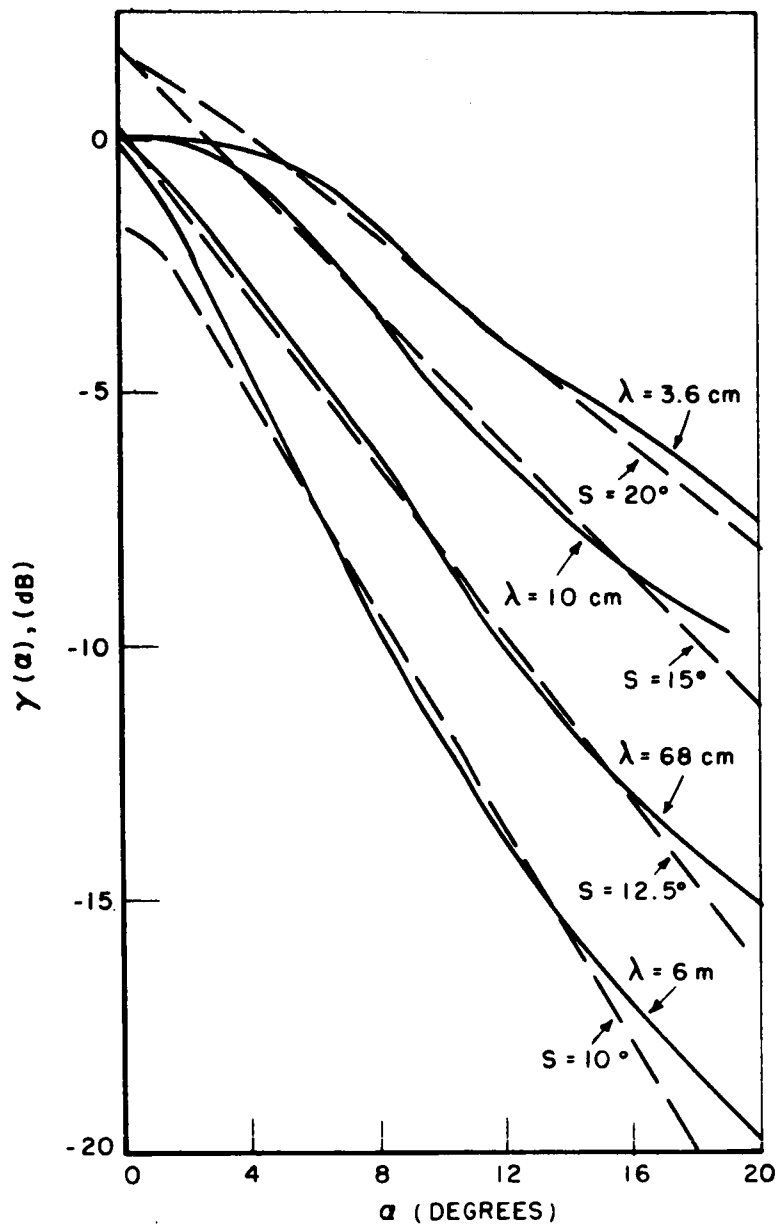


Fig. 16. RMS surface slope, S , as a function of wavelength, λ .

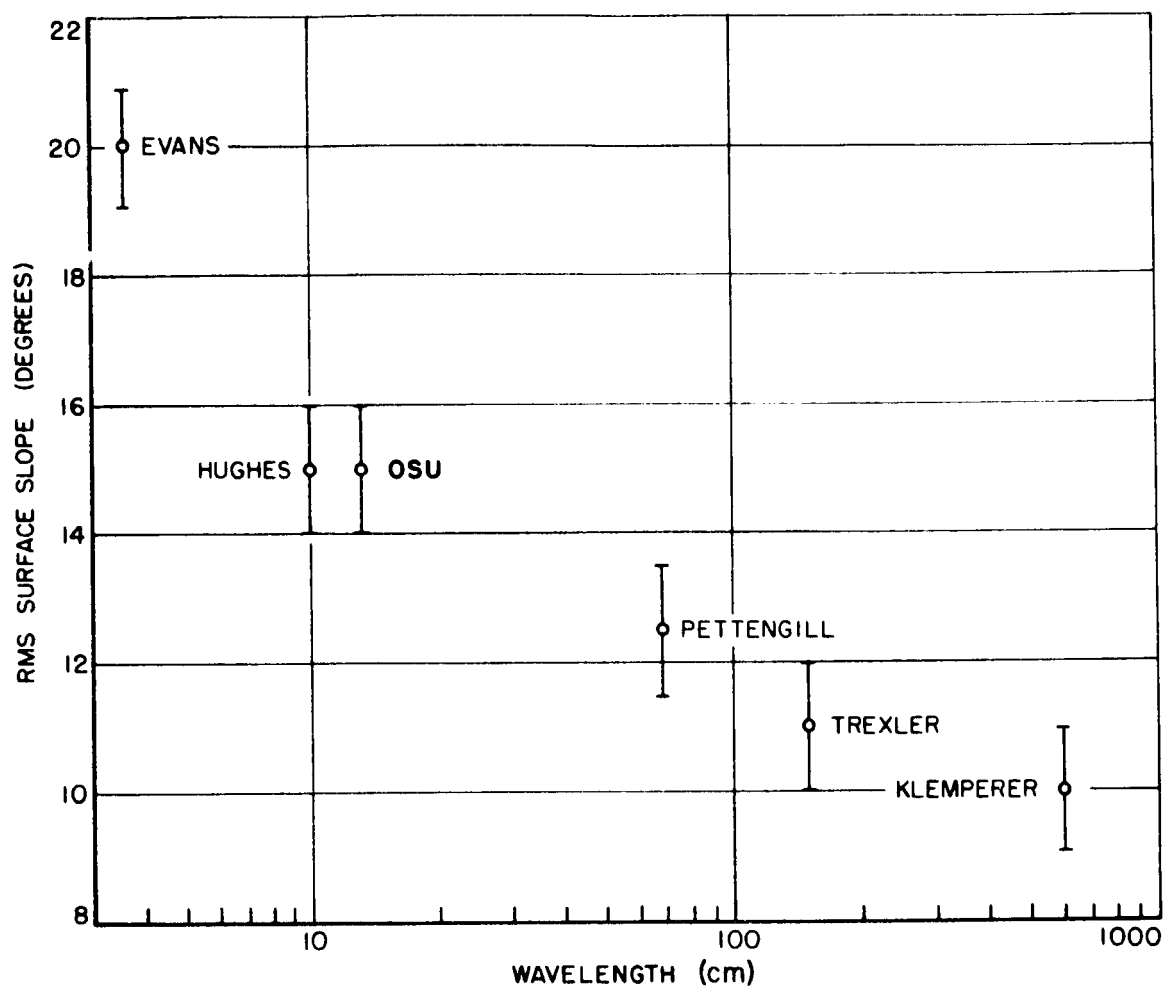


Fig. 17. Frequency dependence of RMS surface slope.

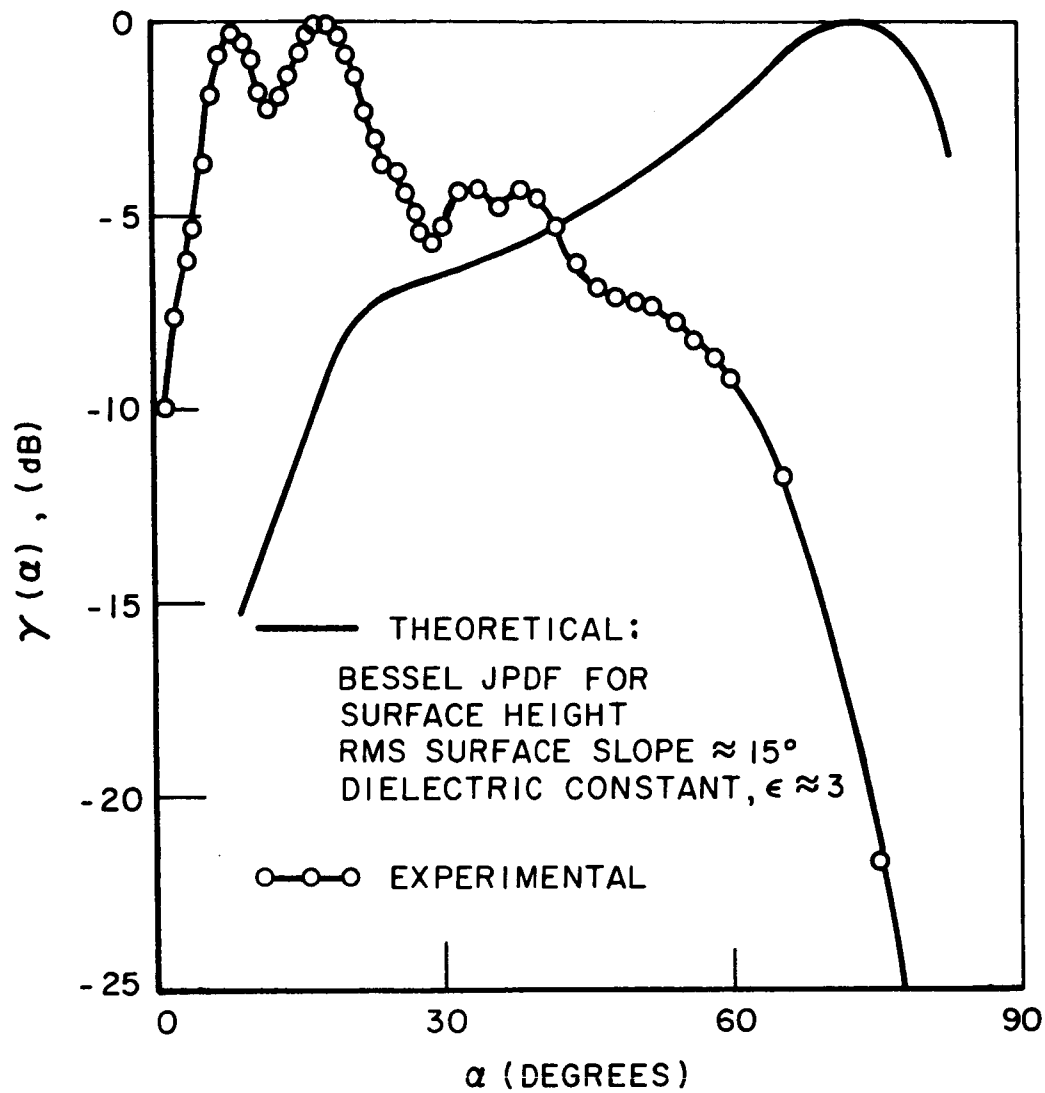


Fig. 18. Comparison of cross-polarized backscattering function with theoretical prediction (Ref. 2, 3).

where

r = radius of the moon,
 d = distance to moon (transmitter-to-moon distance assumed equal to receiver-to-moon distance),
 P_t = transmitted power,
 P_r = received power,
 G_t = transmitter antenna gain,
 G_r = receiver antenna gain,
 λ = wavelength
 g = gain or directivity of the lunar surface, and
 ρ = reflection coefficient.

For the moon, $\pi r^2 = 9.49 \times 10^{12} \text{ m}^2$. For the OU-OSU experiments $d^4 \approx 0.36 \times 10^9 \text{ m}$ (342.2 dB), $P_t G_t = 111 \text{ dBm}$, $G_r = 43 \text{ dBm}$ and $\lambda = 0.132 \text{ m}$ ($\lambda^2 \approx -17.6 \text{ dB}$). The value for P_r , the received power, was estimated using the relation

$$(12) \quad P_r = \frac{S}{N} kT ,$$

where (Fig. 19)

S = area under signal part of the spectrum (watts),
 N = height of the noise level (watts/Hertz),
 k = Boltzmann's constant (1.38×10^{-23} joules/Hz/°K), and
 T = system noise temperature (°K).

The system noise temperature is given by the expression⁸

$$(13) \quad T = 290(NF-1) + T_A ,$$

with NF representing the noise figure and T_A the antenna temperature. The noise level, N , was estimated from the power spectra, such as those shown in Figs. 10 and 11. In some cases, due to the intermodulation noise, there was some difficulty in estimating N .

As a representative example, consider the instance with $NF = 4.35 \text{ dB}$ (2.72) and $T_A = 134^\circ\text{K}$ (south antenna temperature⁸). Then

$$(14) \quad T = 290 (2.72 - 1.0) + 134.0 = 132.8^\circ\text{K}.$$

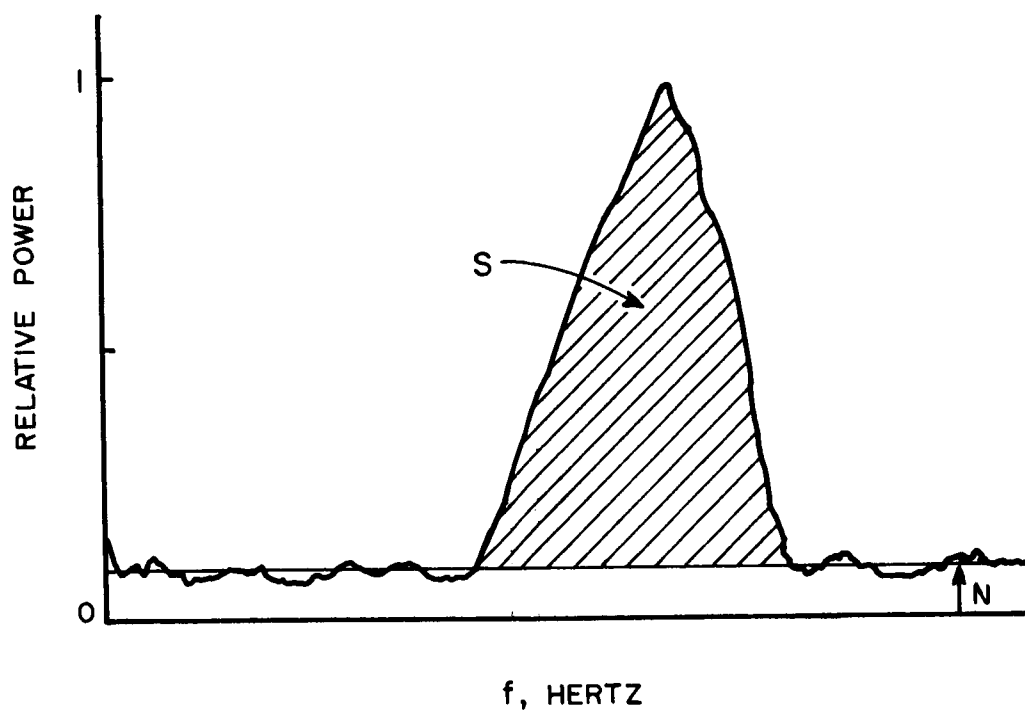


Fig. 19. Estimation of received power, P_r .

With a 2.1 kHz bandwidth (bandwidth of the receivers),

$$(15) \quad kT = (632.8^\circ\text{K}) (1.38 \times 10^{-23} \text{ joules/Hz/}^\circ\text{K}) (2.1 \times 10^3 \text{ kHz}) \\ = 1835 \times 10^{-20} \text{ joules,}$$

or

$$(16) \quad kT = -167.4 \text{ dBw.}$$

Using the data from the south antenna at 19:50 UT on June 3, 1965 as an example, $S = 9.1 \text{ dB}$ and $N = -37.5 \text{ dB}$ so that (see Eq. (12))

$$(17) \quad P_r = 9.1 - (-37.5) + (-167.4) = -120.8 \text{ dBw.}$$

With this value for P_r , Eq. (11) gives, with $(4\pi)^3 = 33.0 \text{ dB}$,

$$(18) \quad \sigma = 33.0 + 342.2 - 120.8 - 111.0 - 43.0 + 17.6 \\ = 118.0 \text{ dB,}$$

or

$$(19) \quad \sigma = 6.3 \times 10^{11} \text{ m}^2.$$

The cross section, expressed as a fraction of the geometrical cross-section, is then

$$(20) \quad g\rho = \frac{\sigma}{\pi r^2} \approx 0.067.$$

During the data runs, data were recorded for half the recording time with one antenna receiving direct- and the other receiving cross-polarized return. The antenna polarizations were then switched and data were recorded during the second half in the opposite mode. For each mode, attenuation was inserted as needed to keep received levels within certain limits. Since, for the present example, the direct-polarized data were attenuated by 18 dB and the

cross-polarized by 3 dB, the difference must be removed in computing the value P_r for the cross-polarized return. Thus using the noise level $N = -37.5$ dB for the south antenna and the value $S = 11.4$ dB, derived from the cross-polarized spectrum at 19:57 UT (see Eq. (12)),

$$(21) \quad P_r = 11.4 - (18 - 3) - (-37.5) - 167.4 = -133.5 \text{ dBw.}$$

Then, just as for the direct-polarized case,

$$(22) \quad \sigma = 33.0 + 342.2 - 133.5 - 111.0 - 43.0 + 17.6 = 105.3 \text{ dB}$$

or

$$(23) \quad \sigma = 0.34 \times 10^{11} \text{ m}^2,$$

and

$$(24) \quad g_p \approx 0.0036.$$

Table I presents the values obtained for the cross section, g_p , for both the direct- and the cross-polarized cases. In Table II values are given for the radar cross section of the moon as reported⁹ by other investigators.

TABLE I
Radar Cross Section of the Moon
at 13.2 cm Wavelength

Date	Time (UT)	$g_{p\text{direct}}$	$g_{p\text{cross}}$
5/4/65	20:12	0.048	-
5/4/65	23:14	.098	-
6/3/65	19:50	.067	0.0036
6/3/65	19:57	.030	.0036
6/3/65	20:20	.062	.0033
	Average	.061	.0035

TABLE II
Radar Cross Section of the Moon as
Reported by Other Investigators

Author	Year	λ (cm)	$g\rho = \frac{\sigma}{\pi r^2}$	Estimated Error (dB)
Lynn	1963	0.86	0.07	± 1
Kobrin	1963	3.0	.07	± 1
Morrow et al	1963	3.6	.07	± 1.5
Evans & Pettengill	1963	3.6	.04	± 3
Kobrin	1963	10.0	.07	± 1
Hughes	1963	10.0	.05	± 3
Victor et al	1961	12.5	.022	± 3
Aarons	1959	33.5	.09	± 3
Blevis & Chapman	1960	61.0	.05	± 3
Fricker et al	1960	73.0	.074	± 1
Leadabrand	1959	75.0	.10	± 3
Trexler	1958	100.0	.07	± 4
Aarons	1959	149.0	.07	± 3
Trexler	1958	150.0	.08	± 4
Webb	1959	199.0	.05	± 3
Evans	1957	250.0	.10	± 3
Evans et al	1959	300.0	.10	± 3
Evans & Ingalls	1962	784.0	.06	± 5
Davis & Rohlf	1964	1130.0	.19	± 3
		1560.0	.13	-2
		1920.0	.16	

The estimation^{1, 9, 11} of the dielectric constant, ϵ , is generally obtained by means of the equation

$$(25) \quad \rho = \left[\frac{1 - \sqrt{\epsilon}}{1 + \sqrt{\epsilon}} \right]^2 ,$$

where ρ is the reflection coefficient. Since ρ is apparently independent of wavelength over the range of wavelengths used for lunar radar experiments, ϵ is assumed real. Equation (25) is exact for a smooth, homogeneous dielectric sphere which is large compared with the wavelength; however its use for the moon must be considered as only a convenient approximation.

Several methods^{1,9} are employed to separate the directivity, g , and the reflection coefficient, ρ . For a smooth isotropically reflecting sphere, $g = 1$; for a Lambert scattering sphere, $g = 8/3$. A value of $g = 1.15$ will be used here. This value was obtained by other investigators¹² from 68 cm data. It is felt that any error introduced by this approximation will be insignificant in comparison with the error in the estimate of the radar cross section, σ , and in consideration of the fact that Eq. (25) is only approximate.

The total cross section, obtained by summing the average of the direct polarized cross section and that of the cross polarized cross section (Table I), is $g\rho \approx 0.0645$. Then, with $g = 1.15$, $\rho \approx 0.056$. Solution of Eq. (25) gives $\epsilon \approx 2.6$. This compares reasonably well with values given by other authors^{9,12} (Evans and Pettengill, $\epsilon = 2.79$ at 68 cm; Muhleman et al, $\epsilon = 2.8$ at 68 cm; Evans and Hagfors, $\epsilon = 2.72$ at 3.6 cm and $\epsilon = 2.13$ at 0.86 cm).

VI. ACCURACY OF MEASUREMENTS

There are many sources of error in an experiment of this complexity. In this section estimates are made of the degrees of error introduced in the various data analysis processes. Analog to digital conversion provided 12 bits of amplitude resolution, or better than 0.2 per cent of full scale accuracy. The error resulting from digitizing the data will thus be considered negligible. In relation to the magnitude of error from other sources, this is not a bad assumption.

The data processing error, up to and including the spectral estimates, is predominantly statistical in nature. This error is due to the fact that only a finite amount of data could be processed. With a frequency resolution of one Hertz and 3 twenty second samples, a precision of ± 2 dB in the estimation of each spectral point was obtained in accordance with the formula (Eq. (7)) discussed in Section V.

The error introduced in computing the backscatter function derives from two sources. The first is the accuracy of the estimate of the limb Doppler values used in frequency normalizing the spectra. The estimates of limb Doppler obtained simply by inspection of the power spectra are thought to be accurate to within ± 0.5 Hertz. This results in negligible error for $\alpha < 45^\circ$ and less than 1 dB for larger α . The computer-derived estimates of limb Doppler are not as accurate. Their computation depends on the accuracy of Ephemeris

data and on the accuracy of the libration computation method (Appendix D), which is a very complex process. The computer estimates found their major application in the selection of data run times and were used only as rough checks on subsequent data analysis.

The second source of error in the backscatter function is the computer program (program 5, Appendix E) which was used to compute $\sigma_0(\alpha)$. By applying the program to certain test functions (Appendix B) it is concluded that the error introduced by the program in computing $\sigma_0(\alpha)$ is less than ± 0.5 dB for $\alpha \leq 60^\circ$.

The error in estimates of σ , the total radar cross section (see Eq. (11), Section V), can be broken down into component errors as follows:

$$\begin{array}{ll} d^4 & \pm 0.2 \text{ dB} \\ G_r & \pm 0.5 \text{ dB} \\ P_t G_r & \pm 2 \text{ dBw} \\ P_r & \pm 2 \text{ dBw} . \end{array}$$

The estimate of error in P_r , the received power, can be broken down further into a ± 0.5 dBw error in the estimate of noise level N and a ± 1.5 dBw error in the value for S (see Eq. (12), Section V). Hence the total error in σ is

$$(26) \quad \text{error}_\sigma = \pm \left[(.2)^2 + (.5)^2 + (2.)^2 + (2.)^2 \right]^{\frac{1}{2}} \\ \approx \pm 3 \text{ dB}.$$

This error estimate is compatible with the variation of the values of $g\rho$ (Table I, Section V) from their averages as well as from the normally accepted value of about 7 per cent.

Using the above error estimate for σ , the possible error in the estimate of the dielectric constant, ϵ , is found by substituting the minimum and maximum values for $g\rho$ into the solution of Eq. (25) (Section V). The resulting limits on ϵ are $2 < \epsilon < 4$, with a most probable value of 2.6.

VII. CONCLUSIONS

On the basis of the results derived from the experiment described in the preceding sections, it may be concluded that the apparent lunar RMS surface slope at a wavelength of 13.2 cm is about 15° ; the lunar radar cross section is approximately 6 per cent for direct polarization and about 0.4 per cent for cross polarization (± 3 dB); and the average dielectric constant of the moon's surface is $\epsilon \approx 2.6$.

By means of the comparison of the experimental backscattering function with that derived theoretically in Reference 2 it may be concluded that the modified Bessel joint probability function serves as a more accurate model for the description of the lunar surface than does the more familiar Gaussian joint probability function.

VIII. RECOMMENDATIONS FOR FUTURE WORK

The experimental results described in the preceding sections, along with the theoretical results of References 2 and 3, represent significant advances in the understanding of the problem of studying planetary surfaces by radar methods. Further studies are needed, however, in the interpretation of the scattering properties of remote surfaces. For example, present interpretation of the lunar surface is based on an arbitrary division of the observed cross-section into two components, a further separation of each component into a directivity and a reflectivity factor, with the reflectivity given by a simple normal incidence Fresnel coefficient. Such a procedure is known to give inconsistent results for terrestrial surfaces, yet is the basis for the "accepted" value of the lunar dielectric constant. It is clear that a study of the diffuse component, in particular, (i. e., return from surfaces with multiple scattering or scattering from edges and cusps) is needed to relate the observed scattering to the geometrical and dielectric properties of the surface. Of particular interest here, for example, would be the use of the depolarized component as a diagnostic of surface roughness, or the interpretation of compound surfaces, where the question of interest is the relation between the fraction of a total surface covered by a given process, and the overall scattering pattern. In short, the apparent success of the single-scattering physical optics approximation should not be allowed to obscure the fact that many surfaces can not be handled that way, and that much study of other scattering mechanisms must be carried out before the problems of remote sensing by radar are solved.

REFERENCES

1. Carpenter, R. L., "Study of Venus by CW Radar — 1964 Results," JPL Technical Report No. 32-963.
2. Barrick, D. E., "A More Exact Theory of Backscattering from Statistically Rough Surfaces," Report 1388-18, 31 August 1965, Antenna Laboratory, The Ohio State University Research Foundation; prepared under Grant No. NsG-213-61 for National Aeronautics and Space Administration.
3. Barrick, D. E., "Theoretical Curves of Backscattering Cross Sections of Rough Surfaces for Several Polarization States Using Two Statistical Models," Report 1388-20, 31 August 1965, Antenna Laboratory, The Ohio State University Research Foundation; prepared under Grant No. NsG-213-61 for National Aeronautics and Space Administration.
4. Compton, R. T., Jr., "The Solution of an Integral Equation for the Lunar Scattering Function," Report 1388-8, 1 April 1963, Antenna Laboratory, The Ohio State University Research Foundation; prepared under Grant No. NsG-213-61 for National Aeronautics and Space Administration.
5. Blackman, R. B. and Tukey, J. W., The Measurement of Power Spectra, Dover, 1958.
6. Turpin, R. H., "Notes on Digital Spectral Analysis," Report 1388-23, 6 February 1967, ElectroScience Laboratory (formerly Antenna Laboratory), The Ohio State University Research Foundation; prepared under Grant No. NsG-213-61 for National Aeronautics and Space Administration.
7. Ott, R. H., "A Theoretical Model for Scattering from Rough Surfaces, with Applications to the Moon and Sea," Report 1388-1, 10 November 1961, Antenna Laboratory, The Ohio State University Research Foundation; prepared under Grant No. NsG-213-61 for National Aeronautics and Space Administration.
8. Hayes, D. E., "System Gain-to-Noise Temperature Ratio Measurements on an Adaptively Phased Array," Report 1963-1, 1 January 1966, Antenna Laboratory, The Ohio State University Research Foundation; prepared under Contract AF 30(602) -3601 for Rome Air Development Center.

9. Evans, J. V., "Radar Studies of the Moon," Radio Science, Vol. 69D, No. 12, December 1965, Sec. D., Journal of Research, National Bureau of Standards.
10. Papoulis, A., Probability, Random Variables, and Stochastic Processes, McGraw-Hill, 1965.
11. Muhleman, D. O., et al., "A Review of Radar Astronomy — Part 1," IEEE Spectrum, October 1965.
12. Muhleman, D. O., et al., "A Review of Radar Astronomy — Part 2," IEEE Spectrum, November 1965.
13. Lawson, J. L. and Uhlenbeck, G. E., Threshold Signals, McGraw-Hill, 1950.
14. The American Ephemeris and Nautical Almanac, 1965, U.S. Government Printing Office, Washington 25, D. C.
15. Claxton, B. H., and Anderson, R. E., "Lunar Reflection Study," General Electric Company, 20 March 1962.
16. Fricker, S. J., et al, "Characteristics of Moon Reflected UHF Signals," MIT Lincoln Lab. Tech Report No. 187, 22 December 1958.
17. Klemperer, W. K., "Angular Scattering Law for the Moon at 6-Meter Wavelength," Journal of Geophysical Research, vol. 70, No. 15, August 1, 1965.

ACKNOWLEDGMENTS

The authors express their appreciation to Messrs: D. Hayes, K. Reinhard, M. Gordon, D. Landis, D. Henry and F. Cook for the collection of the data.

APPENDIX

A. Completion of "The Solution of an Integral Equation for the Lunar Scattering Function"

In Reference 4 (see also References 1 and 12), the solution to the integral equation

$$(30) \quad F(y) = 2 \int_{\sin^{-1} \frac{y}{R}}^{\frac{\pi}{2}} \gamma_0(\alpha) \frac{R^2 \sin \alpha \cos \alpha}{\sqrt{R^2 \sin^2 \alpha - y^2}} d\alpha$$

is given as

$$(31) \quad \gamma_0(\alpha) = - \frac{2}{\pi R^2} \left[\frac{d}{d\beta} \int_{y=R\sqrt{\beta}}^R \frac{yF(y) dy}{\sqrt{y^2 - R^2\beta}} \right]_{\beta=\sin^2 \alpha},$$

where $F(y)$ is proportional to the lunar power density spectrum produced by the Doppler effect and $\gamma_0(\alpha)$ is the average backscattering cross section per unit projected area. The geometry for the above expressions is shown in Figs. 2, Sec. II.

Equation (31) can be simplified to

$$(32) \quad \gamma_0(\alpha) = - \frac{2}{\pi R} \left[\frac{d}{d\beta} \int_{R\sqrt{\beta}}^R \frac{\frac{y}{R} F\left(\frac{y}{R}\right) d \frac{y}{R}}{\sqrt{\left(\frac{y}{R}\right)^2 - \beta}} \right]_{\beta=\sin^2 \alpha}.$$

Let $\xi = \frac{y}{R}$ to get

$$(33) \quad \gamma_0(\alpha) = - \frac{2}{\pi R} \left[\frac{d}{d\beta} \int_{\sqrt{\beta}}^1 \frac{\xi F(\xi)}{\sqrt{\xi^2 - \beta}} d\xi \right]_{\beta=\sin^2 \alpha}.$$

Differentiating with respect to β

$$(34) \quad \frac{d}{d\beta} \int_{u_o(\beta)}^{u_1(\beta)} g(\xi, \beta) d\xi = g(u_1, \beta) \frac{du_1}{d\beta} - g(u_o, \beta) \frac{du_o}{d\beta} \\ + \int_{u_o(\beta)}^{u_1(\beta)} \frac{\partial}{\partial \beta} g(\xi, \beta) d\xi$$

$$\text{where } u_1(\beta) = 1, u_o(\beta) = \sqrt{\beta} \text{ and } g(\xi, \beta) = \frac{\xi F(\xi)}{\sqrt{\xi^2 - \beta}},$$

Eq. (33) becomes

$$(35) \quad \gamma_o(\alpha) = - \frac{2}{\pi R} \left[\frac{1}{2} \int_{\sqrt{\beta}}^1 \frac{\xi F(\xi)}{(\xi^2 - \beta)^{\frac{3}{2}}} d\xi - \frac{1}{2\sqrt{\beta}} \frac{\xi F(\xi)}{\sqrt{\xi^2 - \beta}} \right]_{\xi=\sqrt{\beta}}^1 \Big|_{\beta=\sin^2 \alpha}.$$

Integrating by parts,

$$(36) \quad \int_{\beta}^1 \frac{\xi F(\xi)}{(\xi^2 - \beta)^{\frac{3}{2}}} d\xi = - \frac{F(\xi)}{\sqrt{\xi^2 - \beta}} \Big|_{\xi=\sqrt{\beta}}^1 + \int_{\sqrt{\beta}}^1 \frac{F'(\xi)}{\sqrt{\xi^2 - \beta}} d\xi.$$

Substituting this result into Eq. (35),

$$(37) \quad \gamma_o(\alpha) = - \frac{2}{\pi R} \left\{ \frac{1}{2} \int_{\sqrt{\beta}}^1 \frac{F'(\xi)}{\sqrt{\xi^2 - \beta}} d\xi - \left[\frac{1}{2} \frac{F(\xi)}{\sqrt{\xi^2 - \beta}} \right]_{\sqrt{\beta}}^1 \right. \\ \left. - \frac{1}{2\sqrt{\beta}} \frac{\xi F(\xi)}{\sqrt{\xi^2 - \beta}} \Big|_{\xi=\sqrt{\beta}} \right\} \Big|_{\beta=\sin^2 \alpha}.$$

Assuming $F(1) = 0$ (i. e., the power density at the limb of the moon is zero) and noting that the lower limit of the second term is of equal magnitude and opposite sign compared with the third term, this becomes

$$\gamma_0(\alpha) = \frac{1}{\pi R} \int_{\sqrt{\beta}}^1 \frac{F'(\xi)}{\sqrt{\xi^2 - \beta}} d\xi \Big|_{\beta = \sin^2 \alpha}$$

or

$$(38) \quad \gamma_0(\alpha) = -\frac{1}{\pi R} \int_{\sin \alpha}^1 \frac{F'(\xi)}{\sqrt{\xi^2 - \sin^2 \alpha}} d\xi.$$

From this result and the relation

$$\sigma_0(\alpha) = \gamma_0(\alpha) \cos \alpha,$$

the backscatter cross section per unit area, $\sigma_0(\alpha)$, is given by

$$(39) \quad \sigma_0(\alpha) = \frac{\cos \alpha}{\pi R} \int_1^{\sin \alpha} \frac{F'(\xi)}{\sqrt{\xi^2 - \sin^2 \alpha}} d\xi.$$

B. Empirical $P(f)$ - $\sigma_0(\alpha)$ Pairs*

There are several functions $\sigma_0(\alpha)$ which satisfy the following conditions:

- (1) $0 \leq \sigma_0(\alpha) \leq 1$, $0 \leq |\alpha| \leq \frac{\pi}{2}$;
- (2) $\sigma_0(\alpha) = \sigma_0(-\alpha)$;
- (3) $\sigma_0(\alpha)$ is monotone decreasing for $0 \leq |\alpha| \leq \frac{\pi}{2}$; and
- (4) there is a closed form solution for the integral

* Prepared with assistance of Dr. L. J. Du.

$$(40) \quad P(f) = \int_{\sin^{-1} f}^{\frac{\pi}{2}} \frac{\sigma_o(\alpha) \sin \alpha \, d\alpha}{\sqrt{\sin^2 \alpha - f^2}} .$$

Such functions are of interest from the standpoint that they may provide an insight into the interpretation of experimentally derived backscatter functions.

A number of functions which satisfy the above criteria are given in Table III. These functions were used in testing the computer program for evaluating Eq. (10) of Section V (program 5, Appendix E). Curves for the functions of Table III are given in Figs. 20 and 21. It should be pointed out that in order for the computed $\sigma_o(\alpha)$ to behave properly at $\alpha = \frac{\pi}{2}$, the corresponding function $P(f)$ must satisfy the equation

$$(41) \quad \lim_{f \rightarrow 1} P(f) = 0.$$

It is noted that $P(f)$ of the function pair 5 in Table III does not satisfy this requirement, hence its use as a program check is questionable. It may also be pointed out, however, that the corresponding $\sigma_o(\alpha)$ with $\alpha = 15^\circ$ and $\alpha = 20^\circ$ more nearly approximate the shape of the experimental backscatter function than do the other test functions. The average experimental backscatter function (Fig. 13, Section V) is repeated in Fig. 21 to provide a comparison.

The points in Figs. 20(a) and 21(a) were computed by program 5 (Appendix E) from each function $P(f)$ of Table III. An accuracy of ± 0.5 dB for $\alpha < 70^\circ$ is obtained by comparing the computed points with the empirical curves in Fig. 20(a). All the functions $P(f)$ (Fig. 20(b)) corresponding to these curves satisfy Eq. (41). From Fig. 21(a), an error of less than ± 0.5 dB for $\alpha < 60^\circ$ is achieved for the curves corresponding to $\alpha = 15^\circ$ and $\alpha = 20^\circ$.

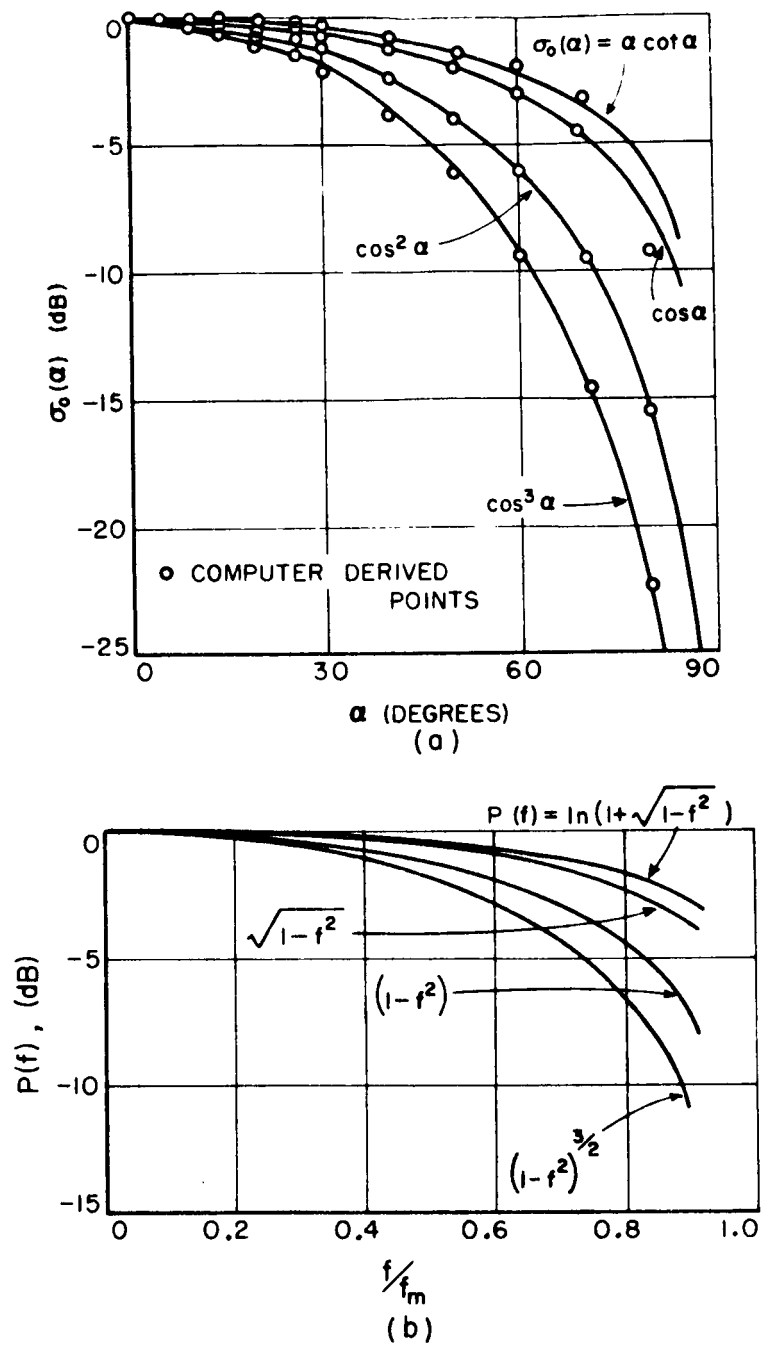


Fig. 20. Empirical $P(f) - \sigma_0(\alpha)$ functional pairs.

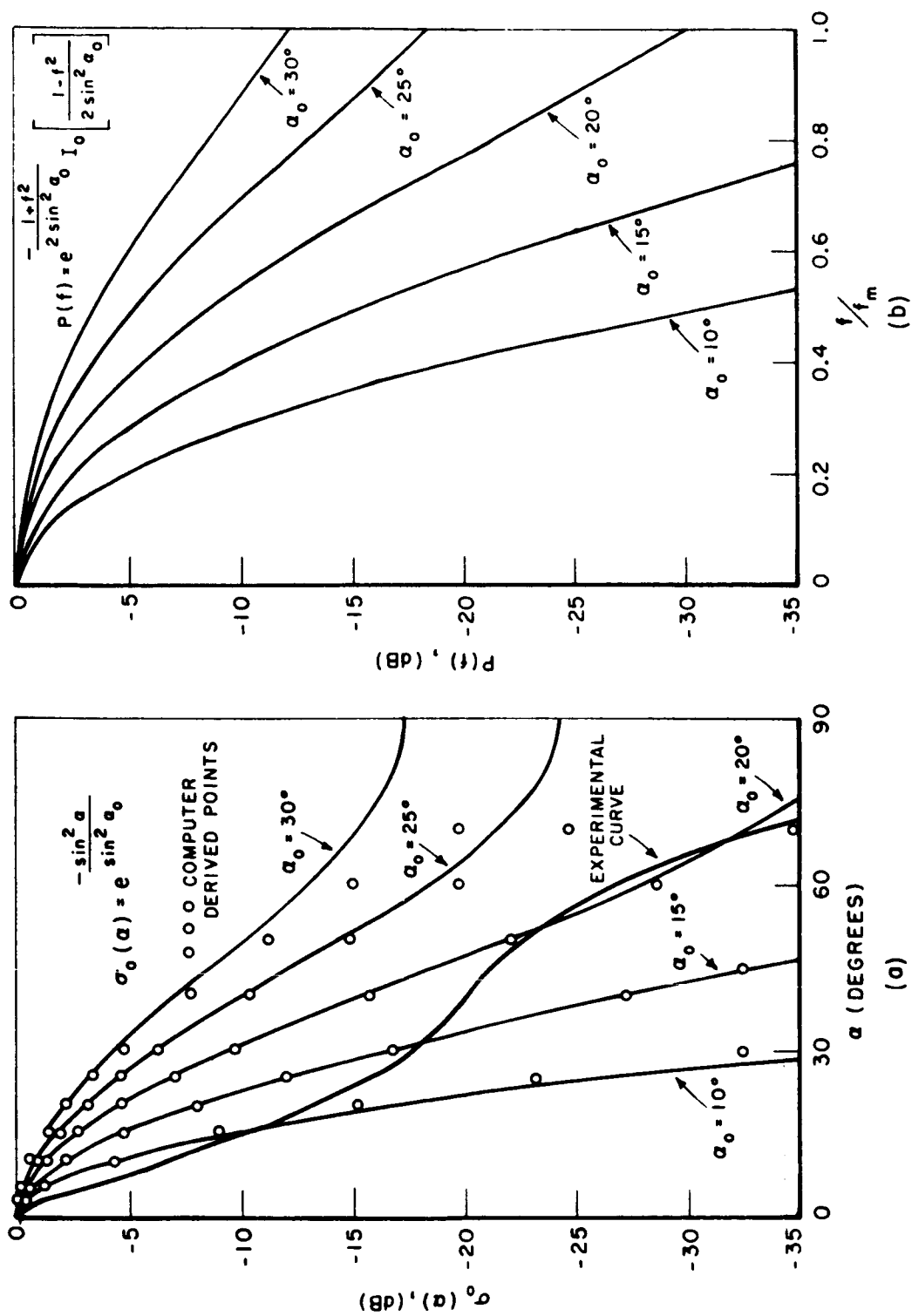


Fig. 21. Empirical $P(f) - \sigma_o(\alpha)$ functional pairs.

TABLE III

	$\sigma_0(\alpha)$	$P(f)^*$
1.	$\alpha \cot \alpha$	$\frac{\pi}{2} \ln(1 + \sqrt{1-f^2})$
2.	$\cos \alpha$	$\sqrt{1-f^2}$
3.	$\cos^2 \alpha$	$\frac{\pi}{4} (1-f^2)$
4.	$\cos^n \alpha$	$\frac{\sqrt{\pi}}{2} \frac{\Gamma(\frac{n+1}{2})}{\Gamma(\frac{n}{2} + 1)} (1-f^2)^{\frac{n}{2}}$
5.	$e^{-\frac{\sin^2 \alpha}{\sin^2 \alpha_0}}$	$\frac{\pi}{2} e^{-\frac{1+f^2}{2 \sin^2 \alpha_0}} I_0 \left[\frac{1-f^2}{2 \sin^2 \alpha_0} \right]$

* $I_0[\xi]$ = Modified Bessel Function

C. Discussion of Receiver Setup

The receiver system is shown in Fig. 4, Sec. III of this report. The Collins 75S-3 receiver was used for its narrow IF bandwidth. Frequencies had to be synthesized which were compatible with the Collins. The requirements are:

- (1) Input frequency less than 30 MHz,
- (2) first IF 3.05 MHz \pm 100 kHz, and
- (3) last IF 455 kHz with 2.1 kHz bandwidth.

The first down conversion from 2270 MHz, usually to 30 MHz, was to about 28.5 MHz (the "front end", including the LEL mixer-preamp, has a bandwidth of about 8 MHz).

The reference into the Dymec stabilizer was nominally 30 MHz; call it f_R . The Dymec RF reference was $N_1 N_2 f_R$ ($N_1 N_2$ integers). When phase-locked in the proper operation mode, the Stalo frequency is

$$(42) \quad f_{LO} = N_1 N_2 f_R \pm f_R = f_R (N_1 N_2 \pm 1).$$

The first IF is

$$(43) \quad f_{IF} = f_S - f_{LO_1} = f_S - f_R (N_1 N_2 \pm 1),$$

where f_S is the frequency of the input signal. The mixing signal in the first mixer in the Collins is normally chosen to lie above the incoming signal. Thus,

$$(44) \quad f_{IF_2} = f_R - f_{IF_1} = f_R - [f_S - f_R (N_1 N_2 \pm 1)]$$

or

$$(45) \quad f_{IF_2} = \begin{cases} N_1 N_2 f_R - f_S, & \text{if } -1 \text{ is used;} \\ f_R (N_1 N_2 + 2) - f_S, & \text{if } +1 \text{ is used.} \end{cases}$$

The value of the product of $N_1 N_2$ must be chosen so that all frequency requirements are met. At the same time, N_1 and N_2 must be numbers which can be achieved with frequency multiplier circuits. f_R was chosen to be 31.5702 MHz, and was derived from the Hewlett-Packard Synthesizer driven from the rubidium standard. Also, $N_1 N_2 = 72$. Here $N_1 = 12$ was obtained by using a commercial tripler and quadrupler by Micromega Corporation, and $N_2 = 6$ was derived in the harmonic generator within the Dymec stabilizer. Thus $N_1 f_R = 378.8424$ MHz, the RF reference in the Dymec was 2273.0544 MHz, and the Stalo frequency when phase-locked was

$$(46) \quad f_{LO} = 2273.0544 - 31.5702 = 2241.4842 \text{ MHz.}$$

If the input signal were exactly 2270 MHz, the first IF would be

$$(47) \quad f_{IF_1} = 2270 - f_{LO} = 28.5158 \text{ MHz.}$$

The second IF would then be

$$(48) \quad f_{IF_2} = 31.5702 - 28.5158 = 3.0544 \text{ MHz.}$$

To obtain exactly 455 kHz, and thus to center f_{IF_3} in the receiver pass band,

$$(49) \quad f_{LO_2} = 3.0544 - 0.455 = 2.5994 \text{ MHz.}$$

f_{LO_2} was synthesized in the Rhode and Schwarz frequency synthesizer driven by the rubidium standard. This second local oscillator was offset and varied in accordance with computed values of Doppler shift to give a final IF output frequency of about 150 Hz.

D. Calculation of Doppler Shift and Doppler Smear of Lunar Radar Echos

In tracking the moon two effects of Earth-moon relative motions must be accounted for. The relative motion of the centers of the two bodies produces an overall Doppler frequency shift of the transmitted signal (Fig. 1). The apparent libration of the moon causes a Doppler smear of the signal. The following methods may be used for calculating the Doppler shift and Doppler smear of moon-reflected radar signals. A computer program incorporating these methods is given following the discussion.

1. Doppler Shift

The rate of change in the distance between the center of the moon and the Earth-based observer produces an overall Doppler shift in the transmitted frequency which must be known in order to track the moon. The following is a method for computing this frequency shift, based on References 15 and 16

Referring to Fig. 22, the distance from an observer, A, (transmitter or receiver) to the center of the moon is given by

$$(50) \quad D_a = \sqrt{D_o^2 + R_a^2 - 2R_a D_o \cos \psi},$$

where

D_a = distance from observer at A to center of moon (meters),
 D_o = distance from center of Earth to center of moon (meters),
 R_a = distance between Earth center and observer at A (meters), and
 ψ = angle between D_o and R_a .

Differentiating, the rate of change of D_a is

$$(51) \quad \dot{D}_a = \frac{\dot{D}_o(D_o - R_a \cos \psi) - D_o R_a \frac{d}{dt} (\cos \psi)}{D_a},$$

where $\dot{D}_a = \frac{d}{dt} D_a$ and $\dot{D}_o = \frac{d}{dt} D_o$. D_o is given by

$$(52) \quad D_o = \frac{R_{eq}}{\sin \Pi},$$

where

R_{eq} = equatorial radius of the Earth (6378.388 km)

and

Π = horizontal parallax (tabulated, pp. 52-67 in 1965 Ephemeris).

Then

$$(53) \quad \dot{D}_o = - \frac{R_{eq} \cos \Pi}{\sin^2 \Pi} \frac{d\Pi}{dt}.$$

The angle ψ is determined in terms of the observer's and the moon's positions. Reference is made to Fig. 23, in which the unprimed coordinates relate to the Earth's equatorial plane and the primed coordinates to the moon's orbital plane, to write

$$(54) \quad \cos \psi = \sin \delta_m \sin \phi_a + \cos \phi_a \cos \delta_m \cos(\text{LHA}),$$

where

LHA = local hour angle = $(Y' D) - (Y' C)$,

ϕ_a = geocentric latitude of the observer,

δ_m = declination of the moon (pp. 68-158 in 1965 Ephemeris), and

Y' = ascending node of moon's orbit on celestial equator.

The local hour angle (LHA) is determined¹⁵ as in the example below (page numbers refer to the 1965 American Ephemeris):

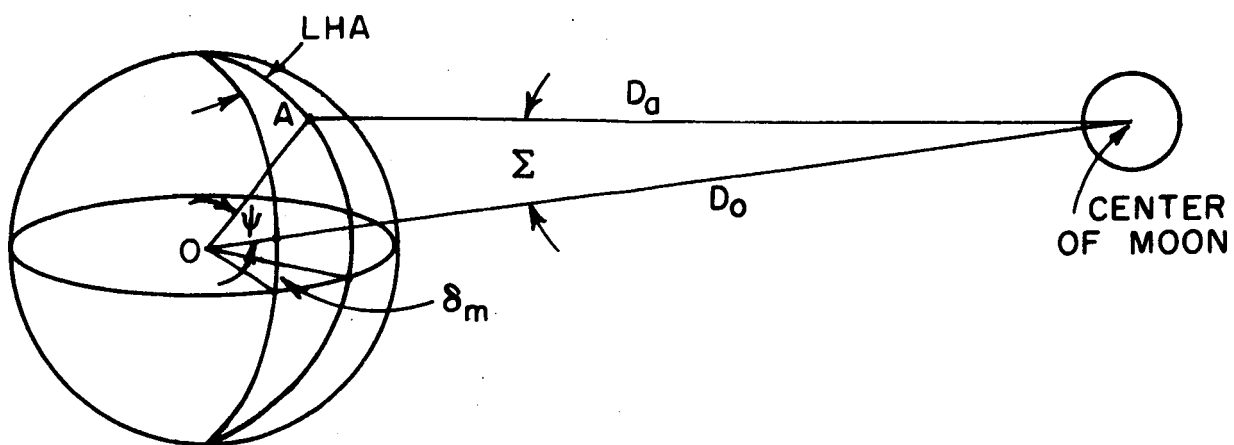


Fig. 22. Geometry for distance from observer to moon.

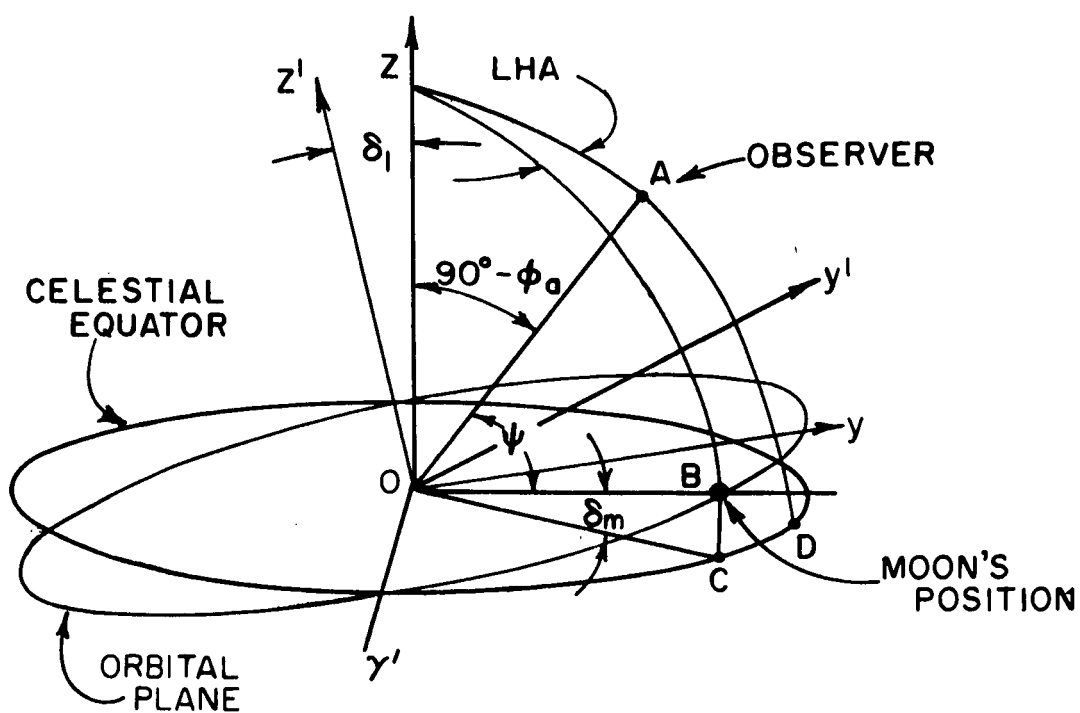


Fig. 23. Geometry for positions of observer and moon.

Station time (UT)*	23 ^h 00 ^m 00.000 ^s
+ Correction factor (UT to Ephemeris Time)	35.000 ^s (p. VII)
- Longitude of station (8 3° 02' 30" W)	- 5 ^h 32 ^m 10.000 ^s
= Local Mean Solar Time	17 ^h 28 ^m 25.000 ^s
Greenwich Mean Sidereal Time (0 ^h UT)	15 ^h 14 ^m 17.164 ^s (p. 12)
+ Correction factor (UT to Ephemeris Time)	35.000 ^s (p. VII)
+ Local Mean Solar Time	17 ^h 28 ^m 25.000 ^s
+ Correction factor (Solar to Sidereal Time)	2 ^m 52.228 ^s (p. 467)
= Local Mean Sidereal Time	32 ^h 46 ^m 9.392 ^s
Local Mean Sidereal Time	32 ^h 46 ^m 9.392 ^s
- Right Ascension	-12 ^h 38 ^m 20.286 ^s (p. 100)
= Local Hour Angle	20 ^h 07 ^m 49.106 ^s

Converting to degrees (15°/hr),

LHA = Local hour angle = -58.05°.

*UT = Universal Time

The geocentric latitude of the observer is given in terms of the corresponding geographic latitude by the expression

$$(55) \quad \tan \phi_a = (1 - e^2) \tan \phi$$

where

ϕ = geographic latitude,
 ϕ_a = geocentric latitude,

and

e = ellipticity of earth ($e^2 = 0.006768658$).

Similarly the radius, R_a , to a point at geocentric latitude ϕ_a is given by

$$(56) \quad R_a^2 = \frac{R_{eq}^2 (1 - e^2)}{1 - e^2 \cos^2 \phi_a}.$$

From Eq. (54),

$$(57) \quad \frac{d}{dt} (\cos \psi) = \dot{\delta}_m [\cos \delta_m \sin \phi_a - \sin \delta_m \cos \phi_a \cos(\text{LHA})] \\ - \frac{d}{dt} (\text{LHA}) \cos \phi_a \cos \delta_m \sin(\text{LHA}),$$

where

$$\dot{\delta}_m = \frac{d}{dt} \delta_m.$$

Letting D_a and D_b represent, respectively, the distances from the transmitter and from the receiver to the center of the moon, the overall Doppler shift is given by

$$(58) \quad f_D = - \frac{f_c}{c} (\dot{D}_a + \dot{D}_b),$$

where

f_D = total Doppler shift (Hz),

f_c = transmitted frequency (Hz),

c = speed of light (m/sec),

\dot{D}_a = relative motion between transmitter and moon center (m/sec),

and

\dot{D}_b = relative motion between receiver and moon center (m/sec).

2. Doppler Smear

To compute the Doppler smear of the spectrum of a transmitted signal it is necessary to compute the libration rate of the moon. There are three sources of lunar libration. A longitudinal libration results from the finite eccentricity of the orbital path. Although the moon rotates on its axis once for each revolution about the Earth, the slight eccentricity coupled with a constant axial rotation produces a "wobble" over the period of a lunar month. A second source of libration is the inclination of the moon's equator to its orbital plane.

A libration in latitude results in this instance. Finally, the motion of an observer on the rotating Earth contributes to the apparent libration of the moon.

Referring to Figs. 24 and 25, the following geometrical relations have been derived:¹⁶

$$(59) \quad \gamma' \gamma = 360^\circ - RA_0$$

where RA_0 is the value of the moon's right ascension during the preceding month at the moment when its declination is zero and increasing. Then

$$(60) \quad \cos \theta = \cos(\gamma' \gamma + RA_m) \cos \delta_m,$$

where RA_m and δ_m are the right ascension and declination, respectively, of the moon at the time of interest. With the angle θ derived from Eq. (60) and the angle

$$(61) \quad S = \frac{1}{2} [\theta + \gamma' \gamma + RA_m + |\delta_m|],$$

we write

$$(62) \quad \delta_i = 2 \sin^{-1} \left[\frac{\sin(S-\theta) \sin(S-\gamma' \gamma - RA_m)}{\sin \theta \sin(\gamma' \gamma + RA_m)} \right]^{\frac{1}{2}}.$$

Then with Ω' , the distance along the celestial equator from the true equinox to the ascending node of the moon's mean equator, interpolated from the Ephemeris (p. 51, 1965 edition),

$$(63) \quad \gamma' \gamma''' = \Omega' + \gamma' \gamma,$$

so that

$$(64) \quad \ell_i = \cos^{-1} [\cos \delta_i \cos i + \sin \delta_i \sin i \cos(\gamma' \gamma''')],$$

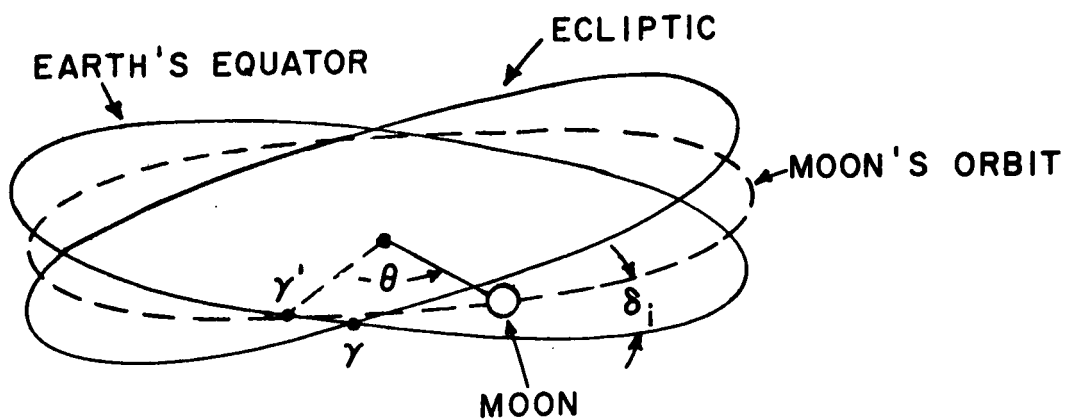


Fig. 24. Geometry for position of the moon.

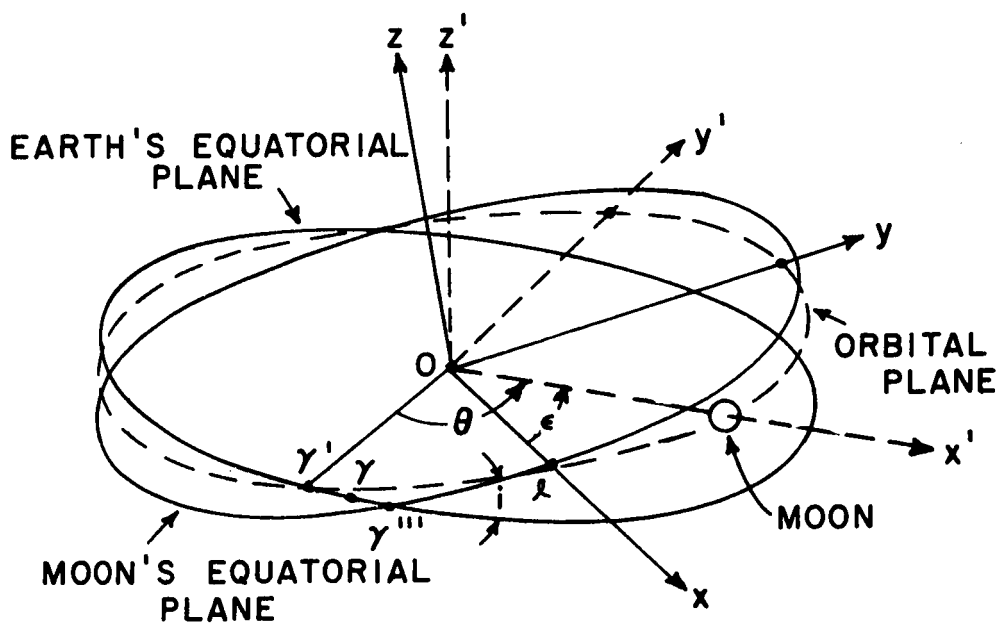


Fig. 25. Orientation of moon.

where i , the inclination of the moon's mean equator to the Earth's true equator, is interpolated from Ephemeris values (p. 51, 1965 edition). Then

$$(65) \quad \gamma' l = \cos^{-1} \left[\frac{\cos \delta_i \cos l_i - \cos i}{\sin \delta_i \sin l_i} \right]$$

and

$$(66) \quad \epsilon = \theta - \gamma' l .$$

The latitudinal and longitudinal libration rates are now computed as follows. Values for the selenographic latitude and longitude, S_β and S_L respectively, are obtained from the Ephemeris (pp. 314 to 321, 1965 edition). Their time derivatives are

$$(67) \quad l_\beta = \frac{d}{dt} S_\beta$$

and

$$(68) \quad l_L = \frac{d}{dt} S_L .$$

The time derivatives of l_β and l_L , i. e., l'_β and l'_L , are the latitudinal and the longitudinal libration rates, respectively, and are given by

$$(69) \quad \begin{aligned} l'_\beta = & \frac{l_\beta}{\sqrt{1 + \cos^2 \epsilon \tan^2 l_i}} - l_L \sin l_i \cos \epsilon \\ & - \left[\frac{S_\beta \cos^2 \epsilon \tan^2 l_i \sec^2 l_i}{(1 + \cos^2 \epsilon \tan^2 l_i)^{\frac{3}{2}}} + S_L \cos \epsilon \cos l_i \right] \frac{dl_i}{dt} \\ & + \left[\frac{S_\beta \cos \epsilon \tan^2 l_i \sin \epsilon}{(1 + \cos^2 \epsilon \tan^2 l_i)^{\frac{3}{2}}} + S_L \sin \epsilon \sin l_i \right] \frac{d\epsilon}{dt} \end{aligned}$$

and

$$\begin{aligned}
(70) \quad l'_L = & \frac{l_\beta \cos \epsilon \tan l_i}{\sqrt{1 + \cos^2 \epsilon \tan^2 l_i}} + l_L \cos l_i \\
& + \left[\frac{S_\beta \cos \epsilon \sec^2 l_i}{(1 + \cos^2 \epsilon \tan^2 l_i)^{\frac{3}{2}}} - S_L \sin l_i \right] \frac{dl_i}{dt} \\
& - \left[\frac{S_\beta \sin \epsilon \tan l_i}{(1 + \cos^2 \epsilon \tan^2 l_i)^{\frac{3}{2}}} \right] \frac{d\epsilon}{dt} ,
\end{aligned}$$

where ϵ is given in Eq. (66) and l_i in Eq. (64).

The parallax angle Σ (Fig. 23) is used to introduce the effect of the observer's motion. The components of Σ are written as

$$\begin{aligned}
(71) \quad \Sigma_L = & \frac{R_a}{D_a} \left\{ \cos \delta_i \cos \delta_m \cos \phi_a \sin(LHA) \right. \\
& \left. - \sin \delta_i [\sin \delta_m \cos \phi_a \cos(\gamma' D) - \cos \delta_m \cos(\gamma' C) \sin \phi_a] \right\}
\end{aligned}$$

and

$$(72) \quad \Sigma_B = \frac{R_a}{D_a} [\sin \delta_i \cos \phi_a \sin(\gamma' D) - \cos \delta_i \sin \phi_a],$$

where R_a (Eq. (56)) is the distance between the Earth's center and the observer at A, D_a (Eq. (50)) is the distance from the observer at A to the moon's center, δ_i is given by Eq. (62) and

$$(73) \quad \gamma' D = LHA + \gamma' C = LHA + \gamma' \gamma + R A_m,$$

where LHA was derived earlier, $\gamma' \gamma$ is given by Eq. (59), and ϕ_a and δ_m are as previously defined. Equations (71) and (72) are differentiated with respect to time to give

$$\begin{aligned}
(74) \quad \dot{\Sigma}_L = & - \frac{\dot{D}_a}{D} \Sigma_L + \omega_e \frac{R_a}{D_a} \cos \phi_a [\cos \delta_i \cos \delta_m \cos(LHA) \\
& + \sin \delta_i \sin \delta_m \sin(Y' D)] \\
& - \frac{d}{dt} (RA_m) \cos \delta_m \frac{R_a}{D_a} [\cos \delta_i \cos \phi_a \cos(LHA) \\
& + \sin \delta_i \sin \phi_a \sin(Y' C)] \\
& - \frac{R_a}{D_a} \dot{\delta}_m \left\{ \sin \delta_m \cos \delta_i \cos \phi_a \sin(LHA) \right. \\
& + \sin \delta_i [\cos \delta_m \cos \phi_a \cos(Y' D) \\
& \left. + \sin \delta_m \cos(Y' C) \sin \phi_a] \right\}
\end{aligned}$$

and

$$(75) \quad \dot{\Sigma}_\beta = - \frac{\dot{D}_a}{D} \Sigma_\beta + \omega_e \frac{R_a}{D_a} \sin \delta_i \cos \phi_a \cos(Y' D),$$

where \dot{D}_a is given in Eq. (51) and ω_e is the angular velocity of the Earth ($\omega_e = 7.2705 \times 10^{-5}$ radians/second).

It is noted¹⁶ that for libration rates not too small ($> 10^{-7}$ radians/sec) Eqs. (74) and (75) may be approximated by ignoring terms including $\dot{\delta}_m$ and $(\dot{D}_a/D_a) \Sigma_{\beta, L}$. In the application of interest to the author, the libration rates were greater than 5×10^{-7} radians/sec, hence Eq. (74) and (75) are simplified to

$$\begin{aligned}
(76) \quad \dot{\Sigma}_L \approx \omega_e \frac{R_a}{D_a} \cos \phi_a [\cos \delta_i \cos \delta_m \cos(LHA) \\
+ \sin \delta_i \sin \delta_m \sin(Y' D)] \\
- \frac{d}{dt} (RA_m) \cos \delta_m \frac{R_a}{D_a} [\cos \delta_i \cos \phi_a \cos(LHA) \\
+ \sin \delta_i \sin \phi_a \sin(Y' C)]
\end{aligned}$$

and

$$(77) \quad \dot{\Sigma}_{\beta} \approx \omega_e \frac{R_a}{D_a} \sin \delta_i \cos \phi_a \cos(\gamma' D) .$$

Having $\dot{\Sigma}_{\beta}$ and $\dot{\Sigma}_L$ for both transmitter and receiver stations, the components of the total libration are given by

$$(78) \quad \ell_{T\beta} = \ell'_{\beta} - \frac{1}{2} (\dot{\Sigma}_{\beta_a} + \dot{\Sigma}_{\beta_b})$$

and

$$(79) \quad \ell_{TL} = \ell'_L - \frac{1}{2} (\dot{\Sigma}_{L_a} + \dot{\Sigma}_{L_b})$$

where the a and b subscripts refer to the transmitter and receiver, respectively. The total libration rate is thus given by

$$(80) \quad \ell_T = \sqrt{\ell_{T\beta}^2 + \ell_{TL}^2} .$$

The libration rate at the point P on the "limb" of the moon as seen by the observer on Earth is (Fig. 26)

$$(81) \quad L = R_m [-\ell_{TL} \cos \alpha + \ell_{T\beta} \sin \alpha] ,$$

where R_m is the radius of the moon. To determine the angle α for which L is a maximum (or minimum), this equation is differentiated and set equal to zero to give

$$(82) \quad \alpha = \tan^{-1} \left[- \frac{\ell_{T\beta}}{\ell_{TL}} \right] .$$

The maximum value of Doppler smear, corresponding to the limb of the moon, is then

$$(83) \quad f_d = \left| \frac{2f_c R_m}{c} (\ell_{T\beta} \sin \alpha - \ell_{TL} \cos \alpha) \right|$$

where c is the velocity of light and f_c the transmitted frequency.

The methods for computing Doppler shift and smear presented here are readily programmed for computer, requiring data from the Ephemeris¹⁴ as well as transmitter and receiver site specifications. The following Scatran computer program applies these methods in computing Doppler shift, Doppler smear and lunar range. In Figs. 27 and 28 are examples of Doppler shift and Doppler smear, respectively, as a function of time (frequency transmitted, 2270 MHz: Transmitter longitude, $82^{\circ} 07' 29''$ W; latitude, $39^{\circ} 19' 28''$ N; receiver longitude, $83^{\circ} 02' 30''$ W; latitude, $40^{\circ} 00' 10''$ N).

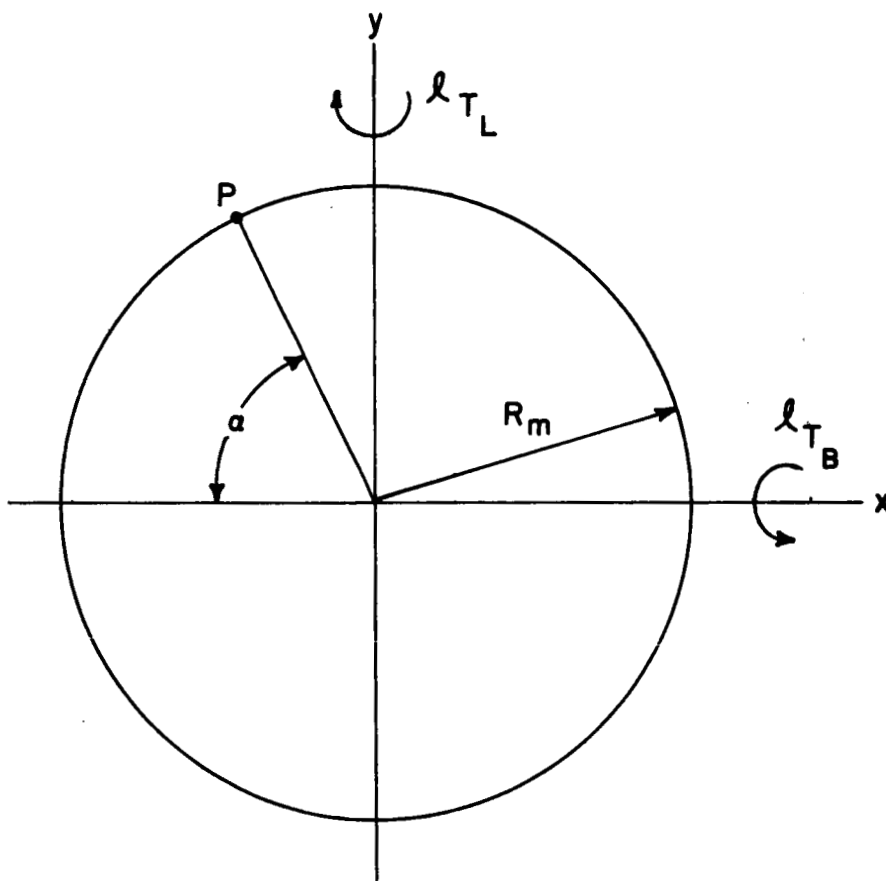


Fig. 26. Geometry for maximum limb Doppler.

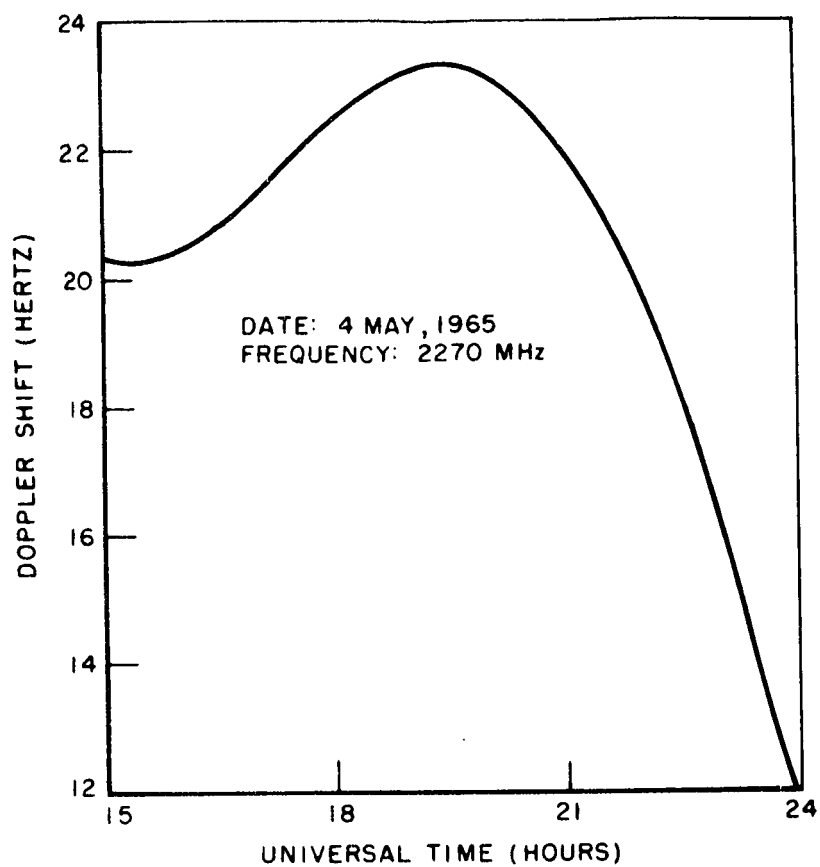


Fig. 27. Doppler frequency shift of transmitted signal.

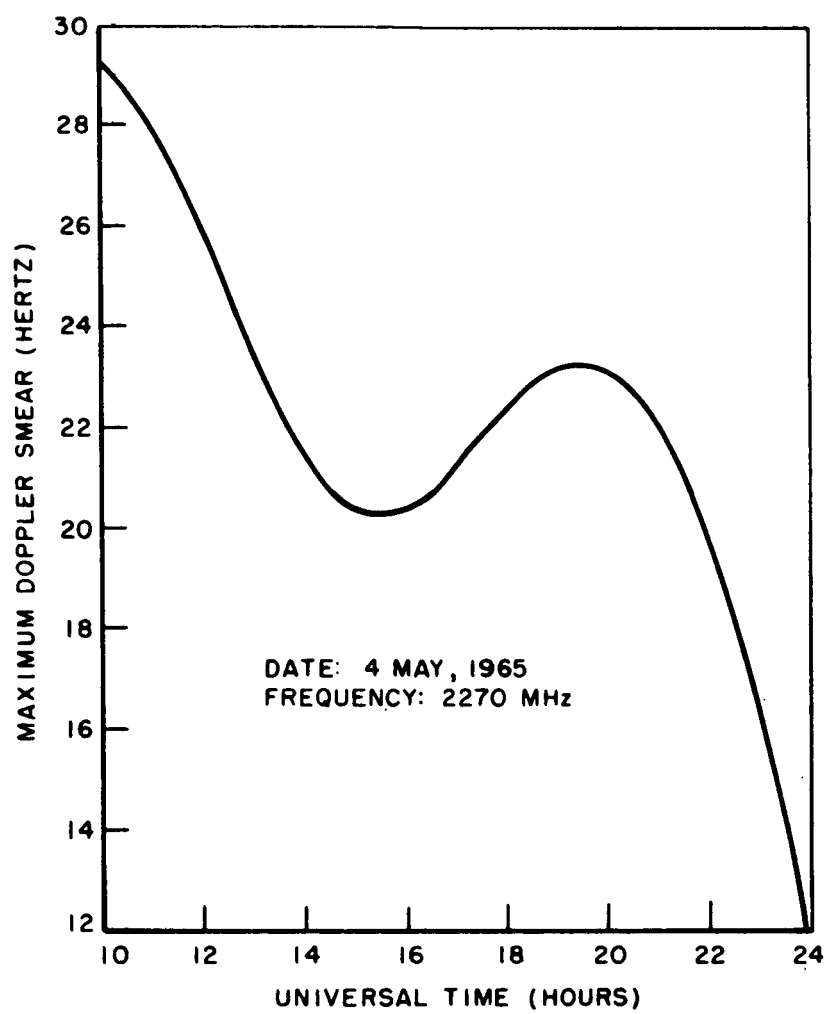


Fig. 28. Doppler smear due to apparent libration.

```

*** RUN,DUMFLOWCORE,SCATRA
C+++++-----
C      6 POINT DIFFERENTIATION
C
C      F = FUNCTION OF X
C      DF = DERIVATIVE OF F WITH RESPECT TO X
C      DELX = SPACING OF EQUALLY-SPACED VARIABLE, X
C      NX = NUMBER OF INTERVALS OF X
C      NX+1 = NUMBER OF VALUES OF X
C
      SUBROUTINE(DF)=DIFF.(F,DELX,NX)-
      DF(0)=(-274*F(0)+600*F(1)-600*F(2)+400*F(3)-150*F(4)+24*F(5))
           /(120*DELX)-
      DF(1)=(-24*F(0)-130*F(1)+240*F(2)-120*F(3)+40*F(4)-6*F(5))
           /(120*DELX)-
      DF(2)=(6*F(0)-60*F(1)-40*F(2)+120*F(3)-30*F(4)+4*F(5))
           /(120*DELX)-
      DO THROUGH(OTHERS),JX=3,1,JX,LE,NX-2-
OTHERS  DF(JX)=(-4*F(JX-3)+30*F(JX-2)-120*F(JX-1)+40*F(JX)
           +60*F(JX+1)-6*F(JX+2))/(120*DELX)-
      DF(NX-1)=(6*F(NX-5)-40*F(NX-4)+120*F(NX-3)-240*F(NX-2)
           +130*F(NX-1)+24*F(NX))/(120*DELX)-
      DF(NX)=(-24*F(NX-5)+150*F(NX-4)-400*F(NX-3)+600*F(NX-2)
           -600*F(NX-1)+274*F(NX))/(120*DELX)-
      NORMAL EXIT-
      END SUBPROGRAM-
C
C+++++-----
C      INTERPOLATION FUNCTION
C
C      F IS DISCRETE FUNCTION WITH NX+1 VALUES OVER X.
C      U IS INTERPOLATED VALUE OF F AT X=XU.
C
      FUNCTION(U)=INTERP.(X,F,NX,XU)-
      H=X(1)-X(0)-
      PROVIDED(XU.GE.X(1)),TRANSFER TO (A1)-
      P=(XU-X(1))/H-
      U=-P*(P-1.)*(P-2.)*F(0)/6 +(P.P.2-1.)*(P-2.)*F(1)/2 -P*(P+1.
           )*(P-2.)*F(2)/2 +P*(P.P.2-1.)*F(3)/6-
      NORMALEXIT-
      A1  PROVIDED(XU.L.X(NX-1)),TRANSFER TO (A2)-
      P=(XU-X(NX-2))/H-
      U=-P*(P-1.)*(P-2.)*F(NX-3)/6 +(P.P.2-1.)*(P-2.)*F(NX-2)/2
           -P*(P+1.)*(P-2.)*F(NX-1)/2 +P*(P.P.2-1.)*F(NX)/6-
      NORMALEXIT-
      A2  DO THROUGH(SEEK),I=1,1,I,L,NX-1-
      SEEK  PROVIDED(XU.GE.X(I).AND.XU.L.X(I+1)),TRANSFER TO (OUT)-
      OUT  P=(XU-X(I))/H-
      U=-P*(P-1.)*(P-2.)*F(I-1)/6 +(P.P.2-1.)*(P-2.)*F(I)/2
           -P*(P+1.)*(P-2.)*F(I+1)/2 +P*(P.P.2-1.)*F(I+2)/6-
      NORMALEXIT-
      ENDSUBPROGRAM-
C
C+++++-----
C      FUNCTION(THETA)=ARCSIN.(X)-
      THETA=90.-(57.3*(1.-X).P.5)*(1.57073-.21211*X+.07426*X.P.2
           -.01873*X.P.3)-
      NORMALEXIT-
      ENDSUBPROGRAM-
C
C+++++-----

```

```

DIMENSION(RA(4),SLO(4),SLA(4),DEC(4),PAR(3),TR(4),TD(4),TP(3),
T(80),RAM(80),DELM(80),LHAA(80),LHAB(80),SELO(80),SELA(80),
DRAM(80),DDELM(80),DPI(80),DSELO(80),DSELA(80),DLHAA(80),DL
HAB(80),EP(80),DEP(80),LI(80),DLI(80),PI(80),DELI(80))-
START READ INPUT,8,(NRUNS)-
READ INPUT,F1,(X1,X2,X3,Y1,Y2,Y3,TEL)-
F F1 (3(F5.0,F3.0,F7.3))-
WRITE OUTPUT,FF1,(X1,X2,X3,Y1,Y2,Y3,TEL)-
F FF1 (58H LUNAR DOPPLER SHIFT, DOPPLER SMEAR AND RANGE COMPUTATIO
NS ///5X,11HTRANSMITTER/10X,F4.,2HHR,F4.,3HMIN,F4.,13HSEC LO
NGITUDE/10X,F4.,3HDEG,F4.,3HMIN,F4.,12HSEC LATITUDE/10X,F5.0,11HM ELE
VATION/)-
TLO=X1+X2/60+X3/3600-
TLA=Y1+Y2/60+Y3/3600-
READ INPUT,F1,(X1,X2,X3,Y1,Y2,Y3,REL)-
WRITE OUTPUT,FF2,(X1,X2,X3,Y1,Y2,Y3,REL)-
F FF2 (5X,8HRECEIVER/10X,F4.,2HHR,F4.,3HMIN,F4.,13HSEC LONGITUDE/1
0X,F4.,3HDEG,F4.,3HMIN,F4.,12HSEC LATITUDE/10X,F5.0,11HM ELE
VATION/)-
RLO=X1+X2/60+X3/3600-
RLA=Y1+Y2/60+Y3/3600-
READ INPUT,F2,(FREQ)-
F F2 (E10.)-
WRITE OUTPUT,FF3,(FREQ)-
F FF3 (5X,10HFREQUENCY=,1PE9.3,2HHZ)-
Z=.01745329-
FLOATING(LI,LPB,LPL,LTB,LT,LHAA,LHAB,LMSTA,LMSTB)-
RADIUS=1.738.X.6-
CONST=2*FREQ*RADIUS/3.X.8-
DO THROUGH(END),NR=1,1,NR.LE.NRUNS-
READ INPUT,F3,(KMO,KDAY,KYR)-
F F3 (3I2)-
WRITE OUTPUT,FF4,(NR,KMO,KDAY,KYR)-
F FF4 (4H1 (.I2,3H) .I2,1H/,I2,1H/,I2/)-
READ INPUT,7,(TMIN,TMAX,DELT)-
READ INPUT,F1,(X1,X2,X3)-
RAO=X1+X2/60+X3/3600-
WRITE OUTPUT,FFRAO,(X1,X2,X3)-
F FFRAO (5H0 RAO /F8.,F4.,F8.3)-
GPG=360.-RAO*15-
NRA=4-
WRITE OUTPUT,FF5-
F FF5 (20H0 RIGHT ASCENSION)-
DO THROUGH(D1),I=0,1,I.L.NRA-
READ INPUT,F4,(TR(I),X1,X2,X3)-
F F4 (F2.,F6.,F4.,F8.3)-
WRITEOUTPUT,FF6,(TR(I),X1,X2,X3)-
F FF6 (5X,F3.,F6.,F4.,F8.3)-
D1 RA(I)=(X1+X2/60+X3/3600)*15-
READ INPUT,F4,(X0,X1,X2,X3)-
WRITE OUTPUT,FF7,(X1,X2,X3)-
F FF7 (33H0 GREENWICH MEAN SIDEREAL TIME/F8.,F4.,F8.3)-
GMST=X1+X2/60+X3/3600-
NDEC=4-
WRITE OUTPUT,FF8-
F FF8 (25H0 APPARENT DECLINATION)-
DO THROUGH(D2),I=0,1,I.L.NDEC-
READ INPUT,F4,(TD(I),X1,X2,X3)-
WRITEOUTPUT,FF6,(TD(I),X1,X2,X3)-
D2 DEC(I)=X1+X2/60+X3/3600-
WRITE OUTPUT,FF9-
F FF9 (24H0 HORIZONTAL PARALLAX)-
DO THROUGH(D3),I=0,1,I.L.3-
READ INPUT,F4,(TP(I),X1,X2,X3)-

```



```

WRITE OUTPUT,FF6,(TP(I),X1,X2,X3)-
D3 PAR(I)=X1+X2/60+X3/3600-
READ INPUT,F5,((SLO(I),SLA(I),I=0,1,1.L.4))-
(8F6.2)-
WRITE OUTPUT,FF10,((SLO(I),SLA(I),I=0,1,1.L.4))-
F FF10 (41H0 SELENOGRAPHIC LONGITUDE AND LATITUDE/(5X,2F10.2))-
READ INPUT,7,(X1,OMEGA)-
WRITE OUTPUT,FF11,(X1,OMEGA)-
F FF11 (7H0 I=.F7.3,11H OMEGA=.F7.3/)-
DO THROUGH(D4),I=0,1,1.L.80-
T(I)=TMIN+I*DELT-
PROVIDED(T(I).E.TMAX),TRANSFER TO (D5)-
D4 CONTINUE-
D5 NT=I-
DO THROUGH(D6),I=0,1,1.LE.NT-
RAM(I)=INTERP.(TR,RA,NRA-1,T(I))-
DELM(I)=INTERP.(TD,DEC,NDEC-1,T(I))-
PI(I)=INTERP.(TP,PAR,2,T(I))-
P=T(I)/24-
X0=-P*(P-1.)*(P-2.)/6-
X1=(P.P.2-1.)*(P-2.)/2-
X2=-P*(P+1.)*(P-2.)/2-
X3=P*(P.P.2-1.)/6-
SELO(I)=X0*SLO(0)+X1*SLO(1)+X2*SLO(2)+X3*SLO(3)-
SELA(I)=X0*SLA(0)+X1*SLA(1)+X2*SLA(2)+X3*SLA(3)-
COSTTA=COS.(Z*(GPG+RAM(I)))*COS.(Z*DELM(I))-
SINTTA=(1.-COSTTA.P.2).P..5-
PROVIDED(COSTTA.LE.1..AND.COSTTA.GE.0.),THETA=90.-ARCSIN.
(COSTTA)-
PROVIDED(COSTTA.L.0..AND.COSTTA.GE.-1.),THETA=90.+ARCSIN.
(-COSTTA)-
S=(THETA+GPG+RAM(I)+.ABS.DELM(I))/2-
X1=SQRT.(SIN.(Z*(S-THETA))*SIN.(Z*(S-GPG-RAM(I)))/(SINTTA*SIN.
(Z*(GPG+RAM(I))))-
PROVIDED(X1.LE.1..AND.X1.GE.0.),DELI(I)=2*ARCSIN.(X1)-
PROVIDED(X1.L.0..AND.X1.GE.-1.),DELI(I)=-2*ARCSIN.(-X1)-
GPG3P=OMEGA+GPG-
X1=COS.(Z*DELI(I))*COS.(Z*X1)+SIN.(Z*DELI(I))*SIN.(Z*X1)*COS.
(Z*GPG3P)-
PROVIDED(X1.LE.1..AND.X1.GE.0.),LI(I)=90.-ARCSIN.(X1)-
PROVIDED(X1.L.0..AND.X1.GE.-1.),LI(I)=90.+ARCSIN.(-X1)-
X1=(COS.(Z*DELI(I))*COS.(Z*LI(I))-COS.(Z*X1))/(SIN.(Z*DELI(I)
)*SIN.(Z*LI(I)))-
PROVIDED(X1.LE.1..AND.X1.GE.0.),GPL=90.-ARCSIN.(X1)-
PROVIDED(X1.L.0..AND.X1.GE.-1.),GPL=90.+ARCSIN.(-X1)-
EP(I)=THETA-GPL-
CORFAC=T(I)*.0027378-
LMSTB=CORFAC+T(I)-RL0+GMST-
LMSTA=CORFAC+T(I)-TL0+GMST-
LHAA(I)=LMSTA*15-RAM(I)-
D6 LHAB(I)=LMSTB*15-RAM(I)-
DELT=DELT*3600-
CALL SUBROUTINE(DRAM)=DIFF.(RAM,DELT,NT)-
CALL SUBROUTINE(DDELM)=DIFF.(DELM,DELT,NT)-
CALL SUBROUTINE(DPI)=DIFF.(PI,DELT,NT)-
CALL SUBROUTINE(DSELO)=DIFF.(SELO,DELT,NT)-
CALL SUBROUTINE(DSELA)=DIFF.(SELA,DELT,NT)-
CALL SUBROUTINE(DLHAA)=DIFF.(LHAA,DELT,NT)-
CALL SUBROUTINE(DLHAB)=DIFF.(LHAB,DELT,NT)-
CALL SUBROUTINE(DLI)=DIFF.(LI,DELT,NT)-
CALL SUBROUTINE(DEP)=DIFF.(EP,DELT,NT)-
STLA=SIN.(Z*TLA)-
CTLA=COS.(Z*TLA)-
SRLA=SIN.(Z*RLA)-

```

F FF12

```

CRLA=COS.(Z*RLA)-
PHI=FATAN1.(.99323134*STLA/CTLA)-
X1=6356756.-
AA=X1/SQRT.(1.-.6763658.X.-2*COS.(PHI).P.2)+TEL-
PHI=FATAN1.(.99323134*SRLA/CRLA)-
AB=X1/SQRT.(1.-.6763658.X.-2*COS.(PHI).P.2)+REL-
WRITE OUTPUT,FF12-
(10H1 TIME,3X,13HDOPPLER SHIFT,3X,13HDOPPLER SMEAR,3X,
12HTRANS. RANGE,3X,12HRECV. RANGE/6X,4HHOUR, 9X,5HHERTZ,
11X,5HHERTZ,10X,6HMETERS, 9X,6HMETERS //)-
DO THROUGH(END),I=0,1,I.LE.NT-
SPI=SIN.(Z*PI(I))-
CPI=COS.(Z*PI(I))-
DO=6378388./SPI-
DDO=-DO*CPI*PI(I)*Z/SP1-
SDELM=SIN.(Z*DELM(I))-
CDELM=COS.(Z*DELM(I))-
SLHAA=SIN.(Z*LHAA(I))-
CLHAA=COS.(Z*LHAA(I))-
SLHAB=SIN.(Z*LHAB(I))-
CLHAB=COS.(Z*LHAB(I))-
COSPSI=SDELM*STLA+CTLA*CDELM*CLHAA-
DCOSPS=DDELM(I)*(CDELM*STLA-SDELM*CTLA*CLHAA)*Z
-CTLA*CDELM*SLHAA*DLHAA(I)*Z-
DA=SQRT.(DO.P.2+AA.P.2-2*AA*DO*COSPSI)-
DDA=(DDO*(DO-AA*COSPSI)-DO*AA*DCOSPS)/DA-
COSPSI=SDELM*SRLA+CRLA*CDELM*CLHAB-
DCOSPS=DDELM(I)*(CDELM*SRLA-SDELM*CRLA*CLHAB)*Z
-CRLA*CDELM*SLHAB*DLHAB(I)*Z-
DB=SQRT.(DO.P.2+AB.P.2-2*AB*DO*COSPSI)-
DDB=(DDO*(DO-AB*COSPSI)-DO*AB*DCOSPS)/DB-
FD=-FREQ*(DDA+DDB)/3.X.8-
SLI=SIN.(Z*LI(I))-
CLI=COS.(Z*LI(I))-
SEP=SIN.(Z*EP(I))-
CEP=COS.(Z*EP(I))-
TANLI=SLI/CLI-
X1=SQRT.(1.+CEP.P.2*TANLI.P.2)-
LPB=Z*DSELA(I)/X1-Z*DSELO(I)*SLI*CEP-(Z*SELA(I)*CEP.P.2*
TANLI.P.2/(CLI.P.2*X1.P.3)+Z*SELO(I)*CEP*CLI)*DLI(I)*Z+
(Z*SELA(I)*CEP*TANLI.P.2*SEP/X1.P.3+Z*SELO(I)*SEP*SLI)
*DEP(I)*Z-
LPL=Z*DSELA(I)*CEP*TANLI/X1+Z*DSELO(I)*CLI+(Z*SELA(I)*CEP/
(CLI.P.2*X1.P.3)-SELO(I)*Z*SLI)*Z*DLI(I)-(Z*SELA(I)*SEP
*TANLI/X1.P.3)*DEP(I)*Z-
SGPDA=SIN.(Z*(LHAA(I)+RAM(I)+GPG))-
CGPDA=COS.(Z*(LHAA(I)+RAM(I)+GPG))-
SGPDB=SIN.(Z*(LHAB(I)+RAM(I)+GPG))-
CGPDB=COS.(Z*(LHAB(I)+RAM(I)+GPG))-
SGPC=SIN.(Z*(RAM(I)+GPG))-
SDELI=SIN.(Z*DELI(I))-
CDELI=COS.(Z*DELI(I))-
DSIGLA=7.2705.X.-5*AA/DA*CTLA*(CDELI*CDELM*CLHAA+SDELI*SGPDA
*SDELM)-DRAM(I)*CDELM*AA/DA*(CDELI*CTLA*CLHAA+SDELI*STLA*SGP
C)*Z-
DSIGBA=7.2705.X.-5*AA/DA*SDELI*CTLA*CGPDA-
DSIGLB=7.2705.X.-5*AB/DB*CRLA*(CDELI*CDELM*CLHAB+SDELI*SGPDB
*SDELM)-DRAM(I)*CDELM*AB/DB*(CDELI*CRLA*CLHAB+SDELI*SRLA*SGP
C)*Z-
DSIGBB=7.2705.X.-5*AB/DB*SDELI*CRLA*CGPDB-
LTB=LPB-.5*(DSIGBA+DSIGBB)-
LTL=LPL-.5*(DSIGLA+DSIGLB)-
XI=FATAN1.(-LTB/LTL)-
DELF=CONST*(LTB*SIN.(X1)-LTL*COS.(X1))-

```

```

END      WRITE OUTPUT,FF13,(T(1),FD,DELF,DA,DB)-
F FF13   (F13.2,F14.2,F14.2,E19.8,E17.8)-
          CALL SUBROUTINE( )=ENDJOB.( )-
          ENDPROGRAM(START)-

```

*** DATA

```

2
05 34 30.000 39 19 28.000 274
05 32 10.000 40 00 10.000 247
2270E6
050465
10.      24.      .25
00 46 55.310
0 05 00 54.869
8 05 21 33.580
16 05 42 27.643
24 06 03 33.320
14 46 76.276
0 22 58 12.530
8 23 48 25.430
16 24 28 15.360
24 24 57 13.430
0 00 59 39.760
12 00 59 43.787
24 00 59 45.238
-3.25 +1.46 -2.15 -0.22 -0.98 -1.90 +0.19 -3.45
23.100 -3.789
060365
10.      24.      .25
00 41 39.776
0 07 51 31.519
8 08 12 50.362
16 08 33 48.627
24 08 54 23.276
16 44 94.937
0 24 32 19.330
8 23 51 58.470
16 23 01 00.430
24 22 00 09.810
0 00 60 23.603
12 00 60 13.416
24 00 60 00.531
-0.31 -3.04 +1.29 -4.49 +2.78 -5.64 +4.07 -6.41
23.062 -3.767

```

E. SCATTRAN Computer Programs (Compatible with the OSU IBM 7094 Computer) for Data Analysis

(1) The data digitized by Wright-Patterson Air Force Base were stored on full digital tapes. This program re-records any of the four channels of data from any portion of the WPAFB tapes. Its purpose is to reduce tape reading time during data analysis.

(2) The data re-recorded by program (1) are smoothed and "decimated"⁵ by the operator $F_2 S_2 S_3$. The mean is removed. The autocovariance and rough spectrum are computed from the modified data. Following the appropriate spectral corrections for the data smoothing, the spectrum is smoothed by Hanning weights.

(3) Data which were digitized at the OSU Computer Center are read by this program, which is compatible with the output of the OSU A/D converter. The data are averaged to determine the mean. The mean is removed if desired (option available by input data card). The autocovariance and rough power spectrum are computed. Hanning weights are used to smooth the spectrum and, by proper choice of option, the spectrum is normalized to its maximum (peak) value. If the spectrum normalizing option is chosen the spectrum may be plotted by selecting the plot option. The plot is the OSU standard Scatran plot performed on the IBM 1620 computer. A card output option is provided for ease in subsequent spectral averaging and for use with program (4).

(4) The center frequency of the lunar spectrum is removed and the spectrum is frequency-normalized to the limb frequency. The card output is compatible with program (5).

(5) From one-sided, frequency-normalized spectra, the average backscattering cross section per unit area, $\sigma_0(\alpha)$ is computed. A card output is provided for later averaging.

(6) A probability density function is computed. The input is compatible with digital tapes from the OSU A/D converter.

**	INPUT	* B01	I LB	TAPE NO. 676
**	OUTPUT	* B02	T HB	SCRATCH TAPE
***	RUN			
***	SCATRAM			
C	PROGRAM NO. 105-T RE-RECORD DATA			
	DIMENSION(IDATA(457),ID(3),ICH(685))-			
START	READ INPUT,8,(NRUNS)-			
	DEFINE POCL,MNDATA,4,690-			
FLIST	FILE LIST(A,\$INPUT \$,\$OUTPUT\$)-			
	ATTACH FILES,MNDATA,A,2-			
	DO THROUGH(DATA),NR=1,1,NR,LE,NRUNS-			
	READ INPUT,FI,(ID(0),ID(1),ID(2))-			
F FI	(I2,I6,I4)-			
	READ INPUT,8,(NRSKIP,NRREAD)-			
	WRITE OUTPUT,FFI,(NR,ID(0),ID(1),ID(2),NRSKIP,NRREAD)-			
F FFI	(2H (.I1,3H) .I2,I6,I4,10H SKIP .I4,15H RECORDS, READ .			
	I3,8H RECORDS/)-			
	DO THROUGH(SKIP),I=1,1,I,LE,NRSKIP-			
SKIP	READ DECIMAL,A,EOF,FTI-			
F FTI	(456L6)-			
	DO THROUGH(DATA),I=1,1,I,LE,NRREAD-			
	READ DECIMAL,A,EOF,FTI,((IDATA(J),J=1,1,J,LE,456))-			
	K=1-			
	DO THROUGH(KINC),N=1,4,N,LE,453-			
	ICH(K)=(IDATA(N).LS.12).RS.24-			
	ICH(K+1)=(IDATA(N).LS.24).RS.24-			
	ICH(K+2)=(IDATA(N+1).LS.24).RS.24-			
	ICH(K+3)=IDATA(N+2).RS.24-			
	ICH(K+4)=IDATA(N+3).RS.24-			
	ICH(K+5)=(IDATA(N+3).LS.12).RS.24-			
KINC	K=K+6-			
DATA	WRITE BINARY,\$OUTPUT\$,((ICH(K),K=1,1,K,LE,684))-			
	CLOSE UNLOAD,A,2-			
	TRANSFER(OUT)-			
EOF	WRITE OUTPUT,FFEOF-			
F FFEF	(12H END OF FILE)-			
OUT	CALL SUBROUTINE()=ENDJOB.()-			
	END PROGRAM(START)-			
***	DATA			

```

** INPUT      * B01      I HB      TAPE NO. 55
*** RUN
*** SCATRAM
      DIMENSION(ID(3),IX(690),IW(12600),U(500),V(500),F(690))-
START  READ INPUT,8,(NRUNS)-
      DEFINE POOL,DATA,2,700-
FLIST  FILE LIST(A,$INPUT $)-
      ATTACH FILES,DATA,A,1-
      DO THROUGH(END),NR=1,1,NR,LE,NRUNS-
      READ INPUT,F1,(ID(0),ID(1),ID(2),TN,TM,FMIN,FMAX,ICH)-
F F1    (I5,I6,I4,4F5.,J5)-
      WRITE OUTPUT,FF1,(ID(0),ID(1),ID(2),TN,TM,ICH)-
F FF1   (79H1PROGRAM NO. 107-T      SPECTRAL ANALYSIS OF UNDETECTED MO
ON DATA (WITH F2S2S3) //5X,7H RUN NO.,I2,I6,I4,10X,4HTN =,
F4,I,14H SEC., TM =,F3,I,18H SEC., CHANNEL ,I1/-)
      READ INPUT,8,(NRSKIP,NRDATA)-
      DO THROUGH(SKIP),I=1,1,I,LE,NRSKIP-
SKIP    READ BINARY,A,EOF,(IA)-
      DO THROUGH(DATAIN),I=1,1,I,LE,NRDATA-
      READ BINARY,A,EOF,((IX(J),J=0,1,J,L .684))-
      PROVIDED(ICH,E,3),TRANSFER TO (CH3)-
      DO THROUGH(IXCH2),J=0,1,J,L .342-
IXCH2   IX(J)=IX(2*J )-
      TRANSFER(SMOOTH)-
CH3     DO THROUGH(IXCH3),J=0,1,J,L .342-
IXCH3   IX(J)=IX(2*J+1)-
SMOOTH  PROVIDED(I,E,1),TRANSFER TO (FIRST)-
      IW(KW)=(IX0+2*(IX1+IX(0))+IX(1))/6-
      KW=KW+1-
      TRANSFER(SECOND)-
FIRST   KW=0-
SECOND  DO THROUGH(INCKW),L=0,2,L,LE,338-
      IW(KW)=(IX(L)+2*(IX(L+1)+IX(L+2))+IX(L+3))/6-
INCKW   KW=KW+1-
      IX0=IX(340)-
      IX1=IX(341)-
DATAIN  ND=171*NRDATA-1-
      NC=TM*625-
      IAVG=0-
      DO THROUGH(AVG),I=0,1,I,L .ND-
      IAVG=IAVG+IW(I)-
      IAVG=IAVG/ND-
      DO THROUGH(DEBIAS),I=0,1,I,L .ND-
DEBIAS  IW(I)=IW(I)-IAVG-
C ACF
      DO THROUGH(ACF2),J=0,1,J,LE,NC-
      F(J)=J/625.-
      IX(J)=0-
      DO THROUGH(ACF1),K=0,1,K,LE,ND-J-
ACF1    IX(J)=IX(J)+IW(K)*IW(K+J)-
ACF2    IX(J)=(IX(J)/(ND-J ))-
      WRITE OUTPUT,FFACF,((F(J),IX(J),J=0,1,J,LE,NC))-
F FFACF (32H AUTOCOVARANCE OF SMOOTHED DATA //(3(F12,4,I15)))-
      FMI=4*NC*FMIN/1250-
      FMA=4*NC*FMAX/1250-
      NP=FMA-FMI-
C MODPSD
      DO THROUGH(PSD2),J=0,1,J,LE,NP-
      F(J)=.5*(J+FMI)/TM-
      U(J)=0.-
      DO THROUGH(PSD1),K=1,1,K,L,NC-
PSD1    U(J)=U(J)+IX(K)*COS.(K*(J+FMI)*3.1416/NC)-
PSD2    U(J)=2*U(J)+IX(0)+IX(NC)*COS.(3.1416*(J+FMI))-
C RAWPSD

```

```

DO THROUGH(PSD3),I=0,1,I.LE.NP-
PROVIDED(F(I).NE.0.),TRANSFER TO (NEXT)-
U(0)=U(0)/6-
TRANSFER(PSD3)-
NEXT ARG=3.1416*F(I)/1250-
U(I)=(SIN.(ARG).P.4)/((SIN.(3 *ARG).P.2)*(SIN.(2*ARG).P.2))*
U(I)-
PSD3 CONTINUE-
C SMPSD
PSD4 DO THROUGH(PSD4),I=1,1,I.LE.NP-
V(I)=(U(I-1)+U(I+1))/4.+U(I)/2.-
V(0)=(U(0)+U(1))/2.-
V(NP)=(U(NP-1)+U(NP))/2.-
DO THROUGH(TRYV),J=0,1,J.LE.NP-
K=-1-
KINC V K=K+1-
TRANSFER TO (MAXV) PROVIDED (K.F.NP+1)-
TRANSFER TO (KINC V) PROVIDED (V(J).GE.V(K))-
TRYV CONTINUE-
MAXV VMAX=V(J)-
WRITE OUTPUT,FFPSD,((F(I),V(I)/VMAX,I=0,1,I.LE.NP))-
F FFPSD (36H1POWER SPECTRUM (HANNING SMOOTHING) //
(5(F10.2,1PE12.3)))-
PUNCH CARDS,8,(NP)-
PUNCH CARDS,FFC,((F(I),V(I)/VMAX,I=0,1,I.LE.NP))-
F FFC (4(F8.2,1PE10.3))-
END CONTINUE-
CLOSE UNLOAD,A-
TRANSFER(OUT)-
EOF WRITE OUTPUT,FFEOF-
F FFEOF (12H END OF FILE)-
OUT CALL SUBROUTINE(=ENDJOB.()-
END PROGRAM(START)-

*** DATA
1
236505042010 10.0 0.25 0.0312.5 3
20 37

```

```

** INPUT * B01 I HB TAPE NO. 743
*** RUN SCATRAM
PARAMETERS(XDIM,12000,WDIM,510,RECORD,521)-
DIMENSION(IX(XDIM),IW(WDIM),FMT(12),DATA(44))-
START READ INPUT,8,(NTAPE,NSPS,NWR,NCHS,NCH,NF,MEAN,NOPLT,NCARDS
, NONORM)-
PROVIDED(NONORM,E,0),NOPLT=0-
READ INPUT,7,(TN,TM,FMIN,FMAX,TSKIP,SIZAXS)-
WRITE OUTPUT,FSPEC1,(NTAPE,NSPS,NWR,NCH,NCHS,NF)-
F FSPEC1 (9H TAPE NO.,15,5X,15,17H SAMPLES/SEC. ,15,13H WORDS/RECO
RD /5X,12H DATA ON CH. ,12,4H OF ,12,20H CHS., FILE NO. ,
11 /)-
WRITE OUTPUT,FSPEC2,(TN,TM,TSKIP)-
F FSPEC2 (1H ,5X,F4,1,14H SEC. OF DATA.,5X,F3,1,20H SEC. MAX. COV. LA
G.,5X,5H SKIP ,F5,1,13H SEC. TO DATA //)-
READ INPUT,FORMAT,((FMT(I),I=0,1,1,L,12))-
F FORMAT (12L6)-
DEFINE POOL,POOL,2,RECORD-
FLIST FILE LIST(A,$INPUT$)-
ATTACH FILES,POOL,A,1-
DO THROUGH(SKIPFI),I=1,1,I,L,NF-
READ READ DECIMAL,A,SKIPFI,9-
TRANSFER(READ)-
SKIPFI CONTINUE-
WRITE OUTPUT,FILE,(I)-
F FILE (9H FILE NO.,12)-
NRSKIP=TSKIP*NSPS*NCHS/(3*NWR)+.5-
DO THROUGH(SKIP),I=1,1,I,LE,NRSKIP-
SKIP READ DECIMAL,A,EOF,9-
NRDATA=TN*NSPS*NCHS/(3*NWR)+.5-
NJ=3*NWR/NCHS-
K=0-
DO THROUGH(DATAIN),I=1,1,I,LE,NRDATA-
READ DECIMAL,A,EOF,FMT,((IA,IB,IC,ID,(IX(J),J=K,1,J,L,K+NJ))-
DATAIN K=K+NJ-
ND=NRDATA*NJ-1-
NC=TM*NSPS+.0001-
TDATA=1.*ND/NSPS-
WRITE OUTPUT,FTD,(TDATA)-
F FTD (9H TDATA = ,F6,3)-
PROVIDED(MEAN,E,0),TRANSFER TO (ACF)-
DO THROUGH(AVG),I=0,1,I,LE,ND-
AVG IAVG=IAVG+IX(I)-
IAVG=IAVG/(ND+1)-
DO THROUGH(DEBIAS),I=0,1,I,LE,ND-
DEBIAS IX(I)=IX(I)-IAVG-
ACF DO THROUGH(ACF2),J=0,1,J,LE,NC-
IW(J)=0-
DO THROUGH(ACF1),K=0,1,K,LE,ND-J-
ACF1 IW(J)=IW(J)+IX(K)*IX(K+J)-
ACF2 IW(J)=IW(J)/(ND-J)-
MINF=2*NC*FMIN/NSPS+.001-
MAXF=2*NC*FMAX/NSPS+.001-
NP=MAXF-MINF-
RAWPSD DO THROUGH(PSD2),J=0,1,J,LE,NP-
IX(J)=0-
DO THROUGH(PSD1),K=1,1,K,L,NC-
PSD1 IX(J)=IX(J)+IW(K)*COS.(K*(J+MINF)*3.1416/NC)-
PSD2 IX(J)=2*IX(J)+IW(0)+IW(NC)*COS.(3.1416*(J+MINF))-
SMPSD IW(0)=(IX(0)+IX(1))/2-
DO THROUGH(SMOOTH),J=1,1,J,L,NP-
SMOOTH IW(J)=(IX(J-1)+IX(J+1))/4+IX(J)/2-
IW(NP)=(IX(NP-1)+IX(NP))/2-
DO THROUGH(TRY),J=0,1,J,LE,NP-

```



```

K=-1-
KINC K=K+1-
TRANSFER TO (MAXM) PROVIDED(K.E.NP+1)-
TRANSFER TO (KINC) PROVIDED(IW(J).GE.IW(K))-
TRY CONTINUE-
MAXM MAX=IW(J)-
WRITE OUTPUT,3,(MAX)-
PROVIDED(NONORM.E.0),MAX=1-
WRITE OUTPUT,FFPSD,((.5*(1+MINF)/TM ,1.*IW(1)/MAX,I=0,1,I.L
E.NP))-
F FFPSD (36H0POWER SPECTRUM (HANNING SMOOTHING) //(5(F10.2,1PE12.
3)))-
WRITE OUTPUT,FMAXM,((.5*(J+MINF)/TM)-
F FMAXM (13H0MAX. PSD AT ,F6.2,3H HZ )-
PROVIDED(NCARDS.E.0),TRANSFER TO (NOCARD)-
PUNCH CARDS,8,(NP)-
PUNCH CARDS,FFC,((.5*(1+MINF)/TM,1.*IW(1)/MAX,I=0,1,I.LE.NP)
)-
F FFC (4(F8.2,1PE10.3))-
NOCARD PROVIDED(NOPLOT.E.0),TRANSFER TO (END)-
DELF=(FMAX-FMIN)/SIZAXS-
CALL SUBROUTINE( )=PLOTS.(DATA,44,0)-
CALL SUBROUTINE( )=AXIS.(0.,0.,FAXIS,-15,SIZAXS,0.,FMIN,DELF,
1.)-
F FAXIS FREQUENCY (HZ)-
CALL SUBROUTINE( )=AXIS.(0.,0.,FORD,9,10.,90.,-40.,4.,1.25)-
F FORD PSD (DB)-
CALL SUBROUTINE( )=PLOT.(0.,10.,3)-
CALL SUBROUTINE( )=PLOT.(SIZAXS,10.,2)-
CALL SUBROUTINE( )=PLOT.(SIZAXS,0.,2)-
CALL SUBROUTINE( )=PLOT.(SIZAXS,10.,+10.*LOG.(1.*IW(NP)/MAX)/4
,3)-
DELF=SIZAXS/NP-
DO THROUGH(PLOTPTS),I=NP-1,-1,I.GE.0-
PLOTPTS CALL SUBROUTINE( )=PLOT.(I*DELF,10.,+10.*LOG.(1.*IW(I)/MAX)/4.
2)-
X=SIZAXS-4.-
FR=1./(TM*DELF)-
CALL SUBROUTINE( )=PLOT.(X,1.,3)-
CALL SUBROUTINE( )=PLOT.(X,1,25,2)-
CALL SUBROUTINE( )=PLOT.(X+FR,1,25,3)-
CALL SUBROUTINE( )=PLOT.(X+FR,1.,2)-
CALL SUBROUTINE( )=PLOT.(X-.25,1,125,3)-
CALL SUBROUTINE( )=PLOT.(X,1,125,2)-
CALL SUBROUTINE( )=PLOT.(X-.1,1,1,075,2)-
CALL SUBROUTINE( )=PLOT.(X-.1,1,175,2)-
CALL SUBROUTINE( )=PLOT.(X,1,125,2)-
CALL SUBROUTINE( )=PLOT.(X+FR,1,125,3)-
CALL SUBROUTINE( )=PLOT.(X+.1+FR,1,075,2)-
CALL SUBROUTINE( )=PLOT.(X+.1+FR,1,175,2)-
CALL SUBROUTINE( )=PLOT.(X+FR,1,125,2)-
CALL SUBROUTINE( )=PLOT.(X+.25+FR,1,125,2)-
CALL SUBROUTINE( )=SYMBOL.(X+.5+FR,1,06.,14,FFR,0.,20)-
F FFR FREQUENCY RESOLUTION-
CALL SUBROUTINE( )=PLOT.( )-
TRANSFER(END)-
EOF WRITE OUTPUT,FEOF-
F FEOF (12H END OF FILE)-
END CLOSE UNLOAD,A,1-
CALL SUBROUTINE( )=ENDJOB.( )-
END PROGRAM (START)-

```

*** DATA

743	500	500	4	1	2	1	1	0	1	
	5.		.5		.0	250.		30.	25.0	

(N18,3N6,375(C12,S12,S12,S12))

```

*** RUN
*** SCATRAM
C
FUNCTION(PMAX)=MAXMM.(P,NT)-
DO THROUGH(TRY),J=0,1,J.LE,NT-
K=-1-
KINC K=K+1-
TRANSFERTO(MAX)PROVIDED(K.E,NT+1)-
TRANSFERTO(KINC)PROVIDED(P(J).GE.P(K))-
TRY CONTINUE-
MAX PMAX=P(J)-
NORMALEXIT-
ENDSUBPROGRAM-
C
C PROGRAM NO. 110-C FREQUENCY NORMALIZATION OF PSD -
DIMENSION(ID(3),F(510),X(510))-
START READ INPUT,8,(NRUNS)-
DO THROUGH(END),NR=0,1,NR.L,NRUNS-
READ INPUT,FINFO,(ID(0),ID(1),ID(2),NP,FATMAX,FDOP)-
WRITE OUTPUT,FFINFO,(NR+1,ID(0),ID(1),ID(2),FDOP)-
F FINFO (15,16,14,15,2F10,2)-
F FFINFO (51H)PROGRAM NO. 110-C FREQUENCY NORMALIZATION OF PSD //
3H (.11,11H) RUN NO. .12,16,14,10X,21HMAX. DOPPLER SM
EAR = .F4.1 ,3H HZ //)-
READ INPUT,FCARDS,((F(I),X(I),I=0,1,I.LE,NP))-
F FCARDS (4(F8,2,1PE10,3))-
DO THROUGH(NORM),I=0,1,I.LE,NP-
NORM F(I)=(F(I)-FATMAX)/FDOP-
J=0-
DO THROUGH(HERE),I=0,1,I.LE,NP-
PRGYP(E(I).L.-1.0.OR.F(I).G.1.0),TRANSFER TO (HERE)-
X(J)=X(I)-
J=J+1-
HERE CONTINUE-
NX=J-1-
XMAX=MAXMM.(X,NX)-
WRITE OUTPUT,FFPSD,((F(I),X(I)/XMAX,I=0,1,I.LE,NX))-
F FFPSD (81H)POWER SPECTRUM (HANNING SMOOTHING), FREQUENCY NORMALIZ
ED TO MAX. DOPPLER SMEAR // (5(F10,4,F12,4))-
PUNCH CARDS,8,(NX)-
PUNCH CARDS,FCC ,((F(I),X(I)/XMAX,I=NX/2,1,I.LE,NX))-
END PUNCH CARDS,FCC ,((F(I),X(I)/XMAX,I=NX/2,-1,I.GE,0))-
F FCC (10F7,4)-
CALL SUBROUTINE( )=ENDJOB.( )-
END PROGRAM(START)-
*** DATA

```

```

*** RUN,DUMFLOWER CORE,SCATRAM
C+++++-----
C      6 POINT DIFFERENTIATION
C
C      F = FUNCTION OF X
C      DF = DERIVATIVE OF F WITH RESPECT TO X
C      DELX = SPACING OF EQUALLY-SPACED VARIABLE, X
C      NX = NUMBER OF INTERVALS OF X
C      NX+1 = NUMBER OF VALUES OF X
C
SUBROUTINE(DF)=DIFF.(F,DELX,NX)-
DF(0)=(-274*F(0)+600*F(1)-600*F(2)+400*F(3)-150*F(4)+24*F(5))
      /(120*DELX)-
DF(1)=(-24*F(0)-130*F(1)+240*F(2)-120*F(3)+40*F(4)-6*F(5))
      /(120*DELX)-
DF(2)=(6*F(0)-60*F(1)-40*F(2)+120*F(3)-30*F(4)+4*F(5))
      /(120*DELX)-
DO THROUGH(OTHERS),JX=3,1,JX,LE,NX-2-
OTHERS DF(JX)=(-4*F(JX-3)+30*F(JX-2)-120*F(JX-1)+40*F(JX)
      +60*F(JX+1)-6*F(JX+2))/(120*DELX)-
DF(NX-1)=(6*F(NX-5)-40*F(NX-4)+120*F(NX-3)-240*F(NX-2)
      +130*F(NX-1)+24*F(NX))/(120*DELX)-
DF(NX)=(-24*F(NX-5)+150*F(NX-4)-400*F(NX-3)+600*F(NX-2)
      -600*F(NX-1)+274*F(NX))/(120*DELX)-
NORMAL EXIT-
END SUBPROGRAM-
C
C+++++-----
C
C      INTERPOLATION FUNCTION
C
C      F IS DISCRETE FUNCTION WITH NX+1 VALUES OVER X.
C      U IS INTERPOLATED VALUE OF F AT X=XU.
C
FUNCTION(U)=INTERP.(X,F,NX,XU)-
H=X(1)-X(0)-
PROVIDED(XU.GE.X(1)),TRANSFER TO (A1)-
P=(XU-X(1))/H-
U=-P*(P-1.)*(P-2.)*F(0)/6 +(P.P,2-1.)*(P-2.)*F(1)/2 -P*(P+1.
      )*(P-2.)*F(2)/2 +P*(P.P,2-1.)*F(3)/6-
NORMAL EXIT-
A1 PROVIDED(XU.L.X(NX-1)),TRANSFER TO (A2)-
P=(XU-X(NX-2))/H-
U=-P*(P-1.)*(P-2.)*F(NX-3)/6 +(P.P,2-1.)*(P-2.)*F(NX-2)/2
      -P*(P+1.)*(P-2.)*F(NX-1)/2 +P*(P.P,2-1.)*F(NX)/6-
NORMAL EXIT-
A2 DO THROUGH(SEEK),I=1,1,I,LE,NX-1-
SEEK PROVIDED(XU.GE.X(I).AND.XU.L.X(I+1)),TRANSFER TO (OUT)-
OUT P=(XU-X(I))/H-
U=-P*(P-1.)*(P-2.)*F(I-1)/6 +(P.P,2-1.)*(P-2.)*F(I)/2
      -P*(P+1.)*(P-2.)*F(I+1)/2 +P*(P.P,2-1.)*F(I+2)/6-
NORMAL EXIT-
ENDSUBPROGRAM-
C
C+++++-----
C
C      F = INTEG.(A,B,FCT.,M,N)
C      A = LOWER LIMIT
C      B = UPPER LIMIT
C      M = ORDER OF INTEGRATION FORMULA FROM 3 TO 11 M ODD.
C      (M = 3 FOR SIMPSONS RULE)
C      N = NUMBER OF INTERVALS (TAKES NEXT HIGHER EVEN
C      MULTIPLE OF M-1)
C      A,B ARE FLOATING

```

```

C      M,N ARE INTEGERS
C      FCT. IS THE NAME WITH PERIOD OF A LIBRARY FUNCTION
C      OR SOURCE FORMULA OR FUNCTION.
C      FORMULAS FROM - TABLES OF LAGRANGIAN INTERPOLATION
C      COEFFICIENTS - COLUMBIA UNIVERSITY PRESS
C
      FUNCTION(F)=INTEG.(P,Q,U.,IX,N)-
      IJ=6-
      DIMENSION(A(30,IJ),B(6))-
      LITERALS(A,1.0,4.0,A(6),7.0,32.0,12.0,A(12),41.0,216.0,27.0,
      272.0,A(18),989.0,5888.0,-928.0,10496.0,-4540.0,A(24),16067.
      0,106300.0,-48525.0,272400.0,-260550.0,427368.0,B,0.33333333
      .0,044444444,0.0071428571,0.00028218695,0.000016701406)-
      M=IX-
      PROVIDED(M.GE.11),M=11-
      PROVIDED(M.LE.3),M=3-
      K=(N-1)/(M-1)-
      M=M/2-
      H=(Q-P)/(2*M*(K+1))-
      MM=M-1-
      F=0.0-
      DOTHROUGH(XY),J=0,2*M,J.LE.2*K*M-
      DOTHROUGH(XX),L=0,1,L.LE.M-
      XX      F=F+A(MM,L)*U.(P+(J+L)*H)-
      DOTHROUGH(XY),L=M-1,-1,L.GE.0-
      XY      F=F+A(MM,L)*U.(P+(J+2*M-L)*H)-
      F=B(MM)*F*H-
      NORMALEXIT-
      ENDSUBPROGRAM-
C+++++
C
      FORMULA(Y)=INTGRD.(X)=INTERP.(F,DP,NP,X)/((X,P.2-XL,P.2).P..
      5)-
      DIMENSION(F(81),P(81),DP(81),GAMMA(81),ALPHA(81),
      DELDEG(10),XLL(10),E(10),NORDER(10),NINT(10))-
      START  READ INPUT,8,(NRUNS)-
      DO THROUGH(END),NR=1,1,NR.LE.NRUNS-
      READ INPUT,8,(NP,NINTVL)-
      DO THROUGH(IN),I=0,1,I.LE.NINTVL-
      IN      READ INPUT,FINT,(DELDEG(I),XLL(I),E(I),NORDER(I),NINT(I))-
      F FINT  (3F10.5,2I10)-
      XLL(NINTVL)=90.-
      READ INPUT,F1,((F(I),P(I),I=0,1,I.LE.NP))-
      F F1    (10F7.4)-
      WRITE OUTPUT,FIN,((F(I),P(I),I=0,1,I.LE.NP))-
      F FIN   (11H11INPUT DATA // (6F10.5))-
      DO THROUGH(NORMAL),I=0,1,I.LE.NP-
      NORMAL  F(I)=F(I)/F(NP)-
      DELF=F(I)-F(0)-
      CALL SUBROUTINE(DP)=DIFF.(P,DELF,NP)-
      DP(0)=0.-
      J=0-
      DO THROUGH(INT),I=0,1,I.LE.NINTVL-
      DO THROUGH(INT),DEG=XLL(I),DELDEG(I),DEG.L.XLL(I+1)-
      ALPHA(J)=DEG-
      XJ=SIN.(ALPHA(J)*.0174533)-
      EE=E(I)*(1.-XJ)-
      XL=XJ+EE-
      A=INTERP.(F,DP,NP,XJ)-
      B=LN.(1.+EE /XJ+SQRT.(2*EE /XJ+(EE .P.2)/(XJ.P.2)))-
      GAMMA(J)=A*B+(INTERP.(F,DP,NP,XL)-A)/EE *(SQRT.(2*XJ*EE
      +EE .P.2)-XJ*B)-
      GAMMA(J)=(GAMMA(J)+INTEG.(XL,1.,INTGRD.,NORDER(I),NINT(I)))
      *(-COS.(ALPHA(J)*.0174533))-

```

INT	J=J+1-
	NP=J-
	ALPHA(NP)=90.-
	GAMMA(NP)=0.-
	DO THROUGH(TRY),J=0,1,J.LE.NP-
	K=-1-
KINC	K=K+1-
	TRANSFER TO (MAXGAM) PROVIDED (K.E.NP+1)-
	TRANSFER TO (KINC) PROVIDED (GAMMA(J).GE.GAMMA(K))-
TRY	CONTINUE-
MAXGAM	GAMMAX=GAMMA(J)-
	WRITE OUTPUT,FF1,(((ALPHA(I),GAMMA(I)/GAMMAX
	,10.*LOG.(GAMMA(I)/GAMMAX),I=0,1,I.LE.NP))-
F FF1	(1H1,6X,5HALPHA,10X,5HGAMMA,9X,6HLOGGAM//(F12,1,1P2E15,4))-
	WRITE OUTPUT,FF0,((XLL(I),E(I),NORDER(I),NINT(I),I=0,1,
	I.L.NINTVL))-
F FF0	(3IHOXLL E NORDER NINT //(F5,1,F8,4,I7,I10))-
	PUNCH CARDS,8,(NP)-
	PUNCH CARDS,FFC,(((ALPHA(I),GAMMA(I)/GAMMAX,I=0,1,I.LE.NP))-
F FFC	(4(F6,1,1PE12,4))-
END	CONTINUE-
	CALL SUBROUTINE(=ENDJOB.()-
	END PROGRAM(START)-
***	DATA

```

** INPUT * B01 I MB TAPE NO. 848
*** RUN,DUMFLOWCORE,SCATRA
    DIMENSION(IX(380),IPDF(151),FMT(12))-
    START READ INPUT,8,(NTAPE,NSPS,NWR,NCHS,NCH,NF)-
    READ INPUT,7,(TSKIP,TREAD) -
    WRITE OUTPUT,FHEAD,(NTAPE,NSPS,NWR,NCH,NCHS,NF,TSKIP,TREAD)-
F FHEAD (29H PROBABILITY DENSITY FUNCTION//5X,9HTAPE NO. ,I3,5X,I5,1
    7H SAMPLES/SEC. ,I5,I3H WORDS/RECORD /5X,12HDATA ON CH. ,
    I2,4H OF ,I2,20H CHS., FILE NO. ,I1//5X,5HSKIP ,F4,1,I2H
    SEC., READ ,F4,1,5H SEC.///12X,12HX P(X)/) -
    READ INPUT,FORMAT,((FMT(I),I=0,1,I.L,12))-
F FFORMAT (12L6)-
    DEFINE POOL,POOL,2,501-
    FLIST FILE LIST (A,$INPUT $) -
    ATTACH FILES,POOL,A,1-
    DO THROUGH(SKIPFI),I=1,1,I.L,NF-
    TRANSFER (READ)-
    READ READ DECIMAL,A,SKIPFI,9-
    SKIPFI CONTINUE-
    NRSKIP=TSKIP*NSPS*NCHS/(3*NWR)+.5-
    DO THROUGH(SKIP),I=1,1,I.LE,NRSKIP-
    SKIP READ DECIMAL,A,EOF,9-
    NRDATA=TREAD*NSPS*NCHS/(3*NWR)+.5 -
    NJ=3*NWR/NCHS -
    NP=75-
    DO THROUGH(READY),I=0,1,I.LE,2*NP-
    READY IPDF(I)=0-
    DO THROUGH(V3),NR=1,1,NR.LE,NRDATA-
    READ DECIMAL,A,EOF,FMT,((IA,IB,IC,ID,(IX(J),J=1,1,J.LE,NJ))-
    DO THROUGH(V3),I=1,1,I.LE,NJ-
    DO THROUGH(V2),J=0,1,J.LE,NP-
    LIM=J*20-10-
    CONDITIONAL(V3)-
    V0 PROVIDED(IX(I).GE.LIM.AND.IX(I).L.LIM+20) OTHERWISE(V1)-
    IPDF(NP+J)=IPDF(NP+J)+1-
    V1 ORPROVIDED(IX(I).L.-LIM.AND.IX(I).GE.-LIM-20) OTHERWISE(V2)-
    IPDF(NP-J)=IPDF(NP-J)+1-
    ENDCONDITIONAL-
    V2 CONTINUE-
    V3 CONTINUE-
    NX=NRDATA*NJ-
    DO THROUGH(LOWER),J=0,1,J.LE,NP-
    PROVIDED(IPDF(J).NE.0),TRANSFERTO(LIMIT)-
    LOWER CONTINUE-
    LIMIT JL=J-1-
    DO THROUGH(UPPER),J=2*NP,-1,J.GE,NP-
    PROVIDED(IPDF(J).NE.0),TRANSFERTO(LIMIT)-
    UPPER CONTINUE-
    LIMIT JU=J+1-
    DEL=(JU-JL)/2.-
    WRITE OUTPUT,FFPDF,((-1.+(J-JL)/DEL,1.*IPDF(J)/NX,
    J=JL,1,J.LE,JU))-
F FFPDF ( 4X,F11,4,F9,4)-
    TRANSFER (END) -
    EOF WRITE OUTPUT,FEOF-
F FEOF (12H END OF FILE)-
    END CLOSE UNLOAD,A,1-
    CALL SUBROUTINE(=ENDJOB.()-
    END PROGRAM (START)-

*** DATA
    848 500 500 4 1 1
    30. 60.
(N18,3N6,375(C12,S12,S12,S12))

```

F. Suggestions for Efficient Digital Spectral Analysis

Any time a digital spectral analysis is performed high computer expenses can be expected. As an example, the time required by an IBM 7094 to compute a spectral estimate with 1 Hertz resolution (1 second maximum autocovariance lag) from a 20 second sample of data at 500 samples per second is about 10 minutes, the largest share of this time being consumed in computing the autocovariance. Of course, 10 minutes is not a lot of computer time, but the information derived from a 20 second sample of data is not great either. Usually a much greater amount of data is available for analysis, and is needed for accurate results. Also, if higher sample rates or finer frequency resolution are needed, computer time will be even greater. Doubling the sample rate multiplies the computer time by about four. Similarly, a two-fold increase in frequency resolution results in about a four-fold increase in computer time. Any reliable way of reducing computer time should be considered since such conservation would permit the analysis of a greater amount of data within the same expense limits.

A method^{1,9, 10, 11} exists which significantly reduces computer time in spectral analysis even though it requires that more data be analysed for equivalent results. The method, which depends on the "arcsine law",⁹ assumes that the random variable analysed is a normal (Gaussian) process. It may be recalled that, in Section IV (Fig. 6), the lunar signals were shown to closely approximate a normal process. It is not unreasonable to expect other planetary scattering data to satisfy this requirement.

The arcsine law provides a relation between $R_x(\tau)$, the autocorrelation function of a Gaussian process $x(t)$, and $R_y(\tau)$, the autocorrelation function of a function $y(t)$, where $y(t)$ is obtained by submitting $x(t)$ to a hard limiting process so that

$$y(t) = \begin{cases} 1, & x(t) \geq 0 \\ -1, & x(t) < 0. \end{cases}$$

According to the arcsine law,

$$(27) \quad R_y(\tau) = \frac{2}{\pi} \sin^{-1} \frac{R_x(\tau)}{R_x(0)}$$

or

$$(28) \quad R_x(\tau) = R_x(0) \sin \left[\frac{\pi}{2} R_y(\tau) \right] .$$

Hence the autocorrelation of $x(t)$ can be uniquely determined from that of $y(t)$.

The advantage of this process is realized in the fact that substantially less time is required to compute the autocorrelation function of a data sequence composed of plus ones and minus ones (a binary sequence) than to compute that of a 12 bit (24 amplitude levels) sequence (the OSU A/D converter provides 12 bit resolution). Using the example given in Reference 11, about a 7 to 1 reduction in time can be realized by using the binary mode as compared with a 16 bit mode or about a 5 to 1 reduction compared with a 12 bit mode (OSU system). These examples take into account the need to analyse more data in the binary mode to obtain results equivalent to those achieved with higher modes (it is pointed out in Reference 11 that approximately $2\frac{1}{2}$ times more binary data must be analysed to obtain a spectrum as smooth as that derived when the 16 bit mode is used).

It is suggested that the OSU Satellite Communications Facility be equipped to convert and record data in the binary mode, provided spectral analysis is expected to be a part of future experiments. The resulting reduction in analysis costs would make practical the analysis of a greater amount of data with a resultant increase in the reliability of the output information.